SLAC-PUB-2298
March 1979
(M)

QUANTUM CHROMODYNAMICS AND THE DYNAMICS OF HADRONS*

Stanley J. Brodsky
Stanford Linear Accelerator Center
Stanford University, Stanford, California 94305

Abstract

The application of perturbative quantum chromodynamics to the dynamics of hadrons at short distance is reviewed, with particular emphasis on the role of the hadronic bound state. A number of new applications are discussed, including

(a) the modification to QCD scaling violations in structure functions due to hadronic binding;
(b) a discussion of coherence and binding corrections to the gluon and sea-quark distributions;
(c) QCD radiative corrections to dimensional counting rules for exclusive processes and hadronic form factors at large momentum transfer;
(d) generalized counting rules for inclusive processes;
(e) the special role of photon-induced reactions in QCD, especially applications to jet production in photon-photon collisions, and photon production at large transverse momentum.

We also present a short review of the central problems in large p_T hadronic reactions and the distinguishing characteristics of gluon and quark jets.

I. INTRODUCTION

In quantum chromodynamics the fundamental degrees of freedom of hadrons and their interactions are the quanta of quark and gluon fields which obey an exact internal SU(3) symmetry. It is possible (but by no means certain!) that quantum chromodynamics is <u>the</u> theory of the strong interactions in the same sense that quantum electrodynmaics accounts for the electromagnetic interactions. In many ways the present period in theoretical physics parallels the 1930's. Although the structure of quantum electrodynamics was known at that time, the lack of a consistent computational scheme allowed only the simplest (Born approximation) aspects of the theory to be understood. Eventually, with the advent of the covariant renormalization program, the full quantum theory could be developed and tested. For example, the QED prediction for the electron's gyromagnetic ratio including sixth order corrections has been confirmed by experiment to 10 significant figures! The fact that we can understand a

---

* Work supported by the Department of Energy under contract number EY-76-C-03-0515.

Lectures presented at the 1978 La Jolla Institute Summer Workshop on QCD, La Jolla, California, July 31 - August 18, 1978.

fundamental parameter of nature to such precision of course encourages our optimism that there is an analogous local gauge field theoretic basis for hadrons. It is well known that the general structure of QCD meshes remarkably well with the facts of the hadronic world especially quark-based (especially charm) spectroscopy, current algebra, the approximate parton-model structure of large momentum transfer reactions, logarithmic scale violations, the scaling and magnitude of $\sigma(e^+e^- \to \text{hadrons})$, jet-production as well as the narrowness of the Ψ as Υ. However, because of the difficulties of computation, it is difficult to obtain rigorous, quantitative predictions beyond leading order, asymptotic limits.

It is clearly crucial to find critical, unassailable tests of QCD. If there is even one bonafide failure in any area of hadronic phenomena, the theory is wrong.

In these lectures, I will concentrate on the application of QCD to hadron dynamics at short distances, where asymptotic freedom allows a systematic perturbative approach. A main theme of this work will be to systematically incorporate the effects of the hadronic wavefunction in deep inelastic reactions. Although it is conventional to treat the hadron as a classical source of on-shell quarks, there are important dynamical effects due to color coherence and constituent off-shell behavior which modify the usual predictions, and lead to a broader testing ground for QCD. We will also discuss QCD predictions for exculsive processes and form factors at large momentum transfer in which the short distance behavior and the finite compositeness of the hadronic wavefunction play crucial roles.

There are a number of excellent introductory and review articles on quantum chromodynamics that I used in preparing these lectures, especially

"Inelastic Processes in QCD"
Y. L. Dokshitser, D. D'yakanov, S. Troyan[1]

"Jets and QCD"
C. H. Llewellyn Smith[2]

"Applications of QCD"
J. Ellis[3]

"Parton-Model Ideas and QCD"
C. T. Sachrajda,[4]

and the Physical Reports by H. Politzer[5] and W. Marciano and H. Pagels.[6] Some of the new topics discussed here are based on work done in collaboration with others, particularly G. P. Lepage, R. Blankenbecler, C. Carlson, Y. Frishman, T. DeGrand, J. Gunion, H. Lipkin, and C. Sachrajda, and I am grateful for their help.

We begin by reviewing the fundamental principles and assumptions of quantum chromodynamics.[7]

A. Quarks are the fundamental representations of

$$SU(n_f) \otimes SU(3)_C \quad ,$$

i.e.: there are n_f flavors $\otimes$ three colors of quarks.[8] Although the flavor symmetry is broken by the weak and electromagnetic interactions, color symmetry is exact; there is no way to distinguish color - all directions in color space are equivalent.

B. Hadrons are color-less states

$$|M\rangle \sim \sum_{i=1}^{3} |\bar{q}_i q_i\rangle \qquad , \qquad |B\rangle = \sum \epsilon_{ijk} |q_i q_j q_k\rangle \quad (1.1)$$

C. $SU(3)_C$ is an exact <u>local</u> symmetry: rotations in color space can be made independently at any point. The mathematical realization of this is the (Yang-Mills) gauge field theory.

D. The Lagrangian density of QCD is

$$\mathscr{L}_{QCD}(x) = \bar{q}_i(x)\ \gamma^\mu\left(i \frac{\partial}{\partial x_\mu} \delta_{ij} + \frac{g}{2} A^a_\mu(x)\ \lambda^a_{ij}\right) q_j(x)$$

$$- \frac{1}{4}\left(\frac{\partial}{\partial x_\mu} A^a_\nu(x) - \frac{\partial}{\partial x_\nu} A^a_\mu(x) + g\, f_{abc}\, A^b_\mu A^c_\nu\right)^2$$

$$i,j = 1,2,3 \quad ; \quad a = 1,2,\ldots,8 \qquad (1.2)$$

(A quark mass term and sum over flavors is understood.) Here the λ^a are the eight Gell-Mann SU(3) matrices with $Tr[\lambda^a,\lambda^b] = 2\delta^{ab}$ (conventional normalization). We can contrast this with

$$\mathscr{L}_{QED} = \bar{q}(x)\ \gamma^\mu\left(i \frac{\partial}{\partial x_\mu} + eA_\mu(x)\right) q(x)$$

$$- \frac{1}{4}\left(\frac{\partial}{\partial x_\mu} A_\nu(x) - \frac{\partial}{\partial x_\nu} A_\mu(x)\right)^2 \qquad (1.3)$$

We can also use the more compact notation

$$\mathscr{L}_{QCD} = \bar{q}(x)\ \not{D}\ q(x) - \frac{1}{4}\ Tr\ F^2_{\mu\nu} \qquad (1.4)$$

where

$$D_\mu = i\partial_\mu - gA_\mu$$

$$F_{\mu\nu} = \partial_\mu A_\nu - \partial_\nu A_\mu - ig[A_\mu , A_\nu] \qquad (1.5)$$

where $A_\mu \equiv \sum_a \frac{\lambda_a}{2} A_\mu^a$, D_μ and $F_{\mu\nu}$ are 3×3 SU(3) color matrices.

Local gauge invariance and color symmetry follows from the invariance of $\mathscr{L}_{QCD}$ under the general gauge transformation

$$A_\mu(x) \rightarrow U(x)\, A_\mu(x)\, U^{-1} + \frac{i}{g}\, U(x)\, \partial_\mu\, U^{-1}(x)$$

$$q(x) \rightarrow U(x)\, q(x) \qquad (1.6)$$

where U is any unitary matrix $U = \exp i \sum_a \theta_a(x) \frac{\lambda_a}{2}$. Note that F is in general not invariant: $F_{\mu\nu}(x) \rightarrow U(x)\, F_{\mu\nu}(x)\, U^{-1}(x)$ since the field strength, like the gluon field is in the adjoint representation of $SU(3)_{color}$.

The Feynman rules of QCD are similar to QED with the $q\bar{q}g$ coupling

$$\gamma_\mu\, \lambda^a_{ij}\, \frac{g}{2} \; .$$

The tri-gluon and quartic gluon coupling color factors are (see Ref. 9)

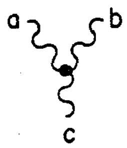

$g\, f_{abc}$

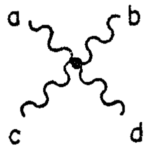

$g^2\, f_{aeb}\, f_{ced} + \cdots$

where $[\lambda^a, \lambda^b] = 2if^{abc}\lambda^c$.

The dimensionless coupling constant is $\alpha_s = g^2/4\pi$. A convenient graphical method for evaluating the color algebra has been given by Cvitanovic.[9] The main rules are

(1) a closed quark loop  gives Tr $[I] = n_c = 3$.

(2) A gluon propagator  is equivalent to 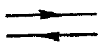 minus $1/n_c$ times the identity (to remove the U_3 singlet). Thus

$$= n_c^2 - 1 = 8$$

(times the coupling constant $\left(\frac{g}{2}\right)^2$ Tr $[\lambda^8 \lambda^8] = g^2/2$.)

Additional rules allow the graphical reduction of the tri-gluon vertex. In typical perturbative calculations (e.g., soft radiation) we have the simple replacement

$$\alpha_{QED} \rightarrow \begin{cases} C_F\,\alpha_s = \frac{4}{3}\alpha_s & \text{quark current} \\ C_A\,\alpha_s = 3\alpha_s & \text{gluon current} \end{cases} \tag{1.7}$$

Effectively "e_g^2" = 9/4 "e_q^2".

Despite the parallels with QED perturbation theory, the postulated absence of asymptotic colored states implies that a perturbative expansion in terms of free - or even dressed - quark and gluon states does not exist in QCD. However, we shall assume that amplitudes with off-shell quark and gluon external legs - corresponding to processes which occur within the hadronic boundaries - do have a perturbative expansion. For such amplitudes, our experience with QED is directly applicable. It is interesting to note that practically all of the predictions recently made for QCD at short distances have a direct analogue in QED, with positronium atoms replacing mesons, etc. In fact, many QCD results for radiative corrections (e.g., structure function moments) and large p_T exclusive or inclusive processes involving bound states actually provide new elegant treatments of QED problems. Conversely, almost every phenomena known in QED and atomic physics has its parallel in QCD.

In my own research in QCD, I always use the criteria of whether a given prediction or approach to hadron dynamics can be carried over to QED. In some cases, one actually finds that a model-dependent assumption used in QCD leads to incorrect results in electrodynamics. Particularly problematic is the often-used device of replacing an incoming hadron by a probabilistic classical distribution of on-shell constituents. This leads to incorrect QED predictions, and, as we shall see, misses interesting hadronic physics.

We normalize the 3-point vertices at a common off-shell (spacelike) mass: $p_i^2 = -\mu^2$, $i = 1,2,3$

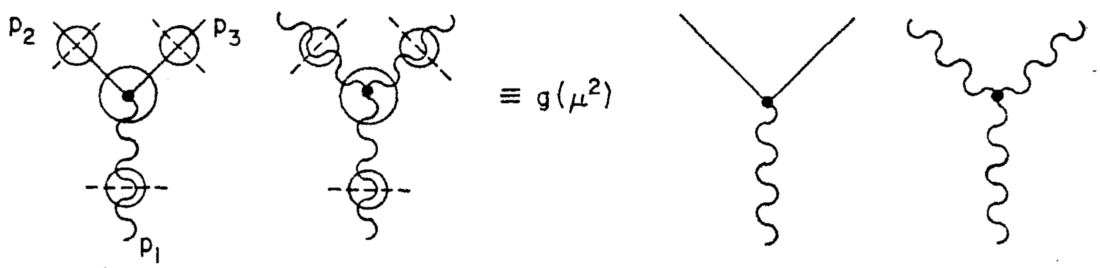

$p_i^2 = -\mu^2$

The circles in the figure indicate vertex and self-energy insertions to all orders. The dividing dotted lines indicate that a square root of propagator renormalization constant is to be associated with "wavefunction" renormalization. Notice that we use the same value of $-\mu^2$ at all legs to keep gauge-invariance for the total Compton amplitude.

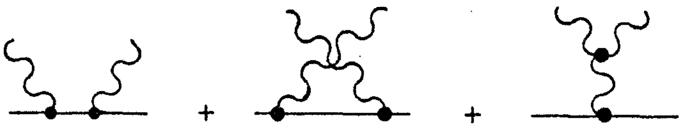

The renormalized amplitude with all vertex and self-energy insertions at $p_i^2 = -\mu^2$ reduces to the Born amplitude with $g^2 = g^2(\mu)$. The choice of μ^2 is arbitrary. Once $\alpha_s(\mu^2)$ is given at any point μ^2, the theory determines α_s at all other values through a renormalization group equation. In terms of diagrams

$$\alpha_s(q^2) = \frac{\alpha_s(\mu^2)}{[1 - \pi(q^2,\mu^2,\alpha_s(\mu^2))]} \tag{1.8}$$

where π is the irreducible gluon self-energy insertion. The lowest order diagrams give ($|q^2|$, $|\mu^2| \gg m_q^2$)

$$\pi^{(2)}(q^2) = \frac{\alpha_s(\mu^2)}{4\pi} \log\left(\frac{-q^2}{\mu^2}\right)\left[\frac{2}{3}n_f + 5 - 16\right] \tag{1.9}$$

where (in the Coulomb gauge) the three terms correspond to the indicated intermediate states.

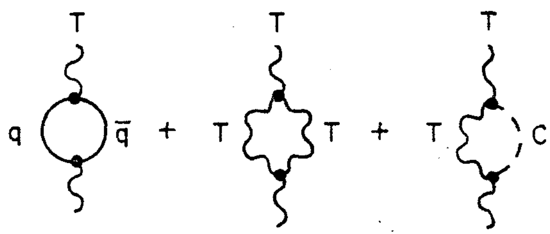

Although the $q\bar{q}$ term must be positive (it is related by unitarity to $e^+e^- \to q\bar{q}$) the crucial Coulomb plus transverse gluon term does not correspond to the production of physical quanta and can indeed be negative.[14]

Thus to lowest order, $\alpha_s(q^2)$ decreases logarithmically (if $n_f \le 16$)

$$\alpha_s(q^2) = \frac{\alpha_s(\mu^2)}{\left[1+\frac{\alpha_s(\mu^2)}{4\pi}\log\frac{-q^2}{\mu^2}\,(11-2/3\;n_f)\right]} \tag{1.10}$$

We shall assume that this is the correct asymptotic limit and verify that the result is self-consistent to all orders. The next order diagrams

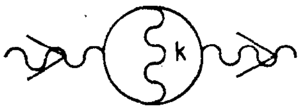

gives, as in QED, $\pi^{(4)} \sim O[\alpha_s^2(\mu^2)\log q^2/\mu^2]$. However, we can include the effects of the self-energy insertions associated with the exchanged gluon by utilizing $\alpha_s(k^2)$: we have the effective replacement:

$$\alpha_s^2(\mu^2)\;\log\frac{q^2}{\mu^2} \Longrightarrow \alpha_s(\mu^2)\int_{\mu^2}^{q^2}\frac{dk^2}{k^2}\,\alpha_s(k^2)$$

$$\sim \alpha_s(\mu^2)\;\log\log q^2 \tag{1.11}$$

assuming $\alpha_s(k^2) \sim 1/\log q^2$ asymptotically. Thus we have

$$\frac{4\pi}{\alpha_s(q^2)} = \frac{4\pi}{\alpha_s(\mu^2)} + (11-2/3\;n_f)\;\log\frac{-q^2}{\mu^2} + O(\log\log q^2) \tag{1.12}$$

It is easy to see that higher order insertions grow even less strongly with q^2, and the original ansatz is indeed self-consistent. The logarithmic decrease of the "running coupling constant" $\alpha_s(q^2)$ indicates that the effective force due to gluon exchange becomes weak at short distance when vertex and self-energy insertions of all orders are accounted for. The effect of these insertions is also to weaken the ultraviolet growth of all loop calculations compared to lowest order perturbation theory.

Unlike QED where α can be fixed directly by Coulomb scattering, the empirical determination of α_s at any renormalization point is non-trivial. It is conventional to use the form

$$\tilde{\alpha}_s(q^2) = \frac{4\pi}{(11-2/3\;n_f)\;\log\frac{-q^2}{\Lambda^2}} \tag{1.13}$$

and attempt to determine Λ^2 phenomenologically. However this form can only be used for $q^2 >> \Lambda^2$ and $\log q^2/\Lambda^2 >> \log\log q^2$; in particular, the pole at $-q^2 = \Lambda^2$ is incorrect. Many analyses unfortunately tend to determine Λ^2 by fitting to the rapid rise of α_s at $q^2 = -\Lambda^2$.

The actual form of α_s can only have singularities at q^2 timelike where the cuts corresponding to gluon and quark production begin. A convenient simple form which moves the pole to $q^2 = 0$ is[15]

$$\tilde{\alpha}_s(q^2) = \frac{4\pi}{(11-2/3\ n_f)\ \log\left(1-\frac{q^2}{\Lambda^2}\right)} \qquad (1.14)$$

or perhaps

$$\frac{4\pi}{\tilde{\alpha}_s(q^2)} = 11\log\left(1-\frac{q^2}{\Lambda^2}\right) - \frac{2}{3}\sum_f \log\left(1-\frac{q^2-4m_f^2}{\Lambda^2}\right) \qquad (1.15)$$

which also takes into account heavy quark thresholds.

An amusing but heuristic feature of the form (1.14) is that it automatically produces a confining linear potential at large distances ($V_{eff} \to C/\vec{q}^{\,4}$, $V_{eff}(r) \to \tilde{C}r$) as well as any asymptotically free form ($V_{eff} \to C'/q^2 \log q^2$, $V_{eff}(r) \sim \tilde{C}'/r \log r$) at short distance. Richardson[15] has shown that using this result as a Schroidinger potential gives an excellent representation of the charm and upsilon spectra. The linear potential agrees with the string model Regge slope $\alpha_R'(0) = 0.90$ GeV^{-2} with $\Lambda = 0.436$ GeV and $n_f = 3$ in Eq. (1.14).

The above speculations on the form of $\alpha_s(q^2)$ are of course only meant to be suggestive. Any non-perturbative effects are expected to be important in the long distance domain. The form of the effective potential between quarks with a hadron is also affected by gluon exchange and retardation effects not included in a naive potential. Further, the gluon and quark pair self-energy insertions in the gluon propagator are themselves effected by higher order corrections, probably giving an effective mass to the gluon intermediate states and weakening the singularity of $\alpha_s(q^2)$ at $q^2 = 0$.

Despite these complexities, there is evidently a unique form for $\alpha_s(q^2)$ determined by the theory.

Another aspect of the non-perturbative nature of QCD is its novel, non-trivial structure of the vacuum state - often described as a dilute gas of instantons (classical solutions of the gauge field sector of the theory). We shall assume that for processes which occur at short distances, i.e.: probe 4-momentum squared Q^2 greater than typical hadronic masses, the non-perturbative effects can be numerically neglected. Estimates of instanton effects which have appeared in the literature support this view.[10] In addition, one can imagine further non-perturbative effects due to initial or final state interactions; e.g., in the Drell-Yan process $pp \to \ell\bar{\ell}X$ the nucleons could influence each other even at large $Q^{\mu} = (\ell + \bar{\ell})^2$. On the other hand, Witten[11] has argued (on the basis of results from soluable gauge field theories) that instantons do not play an important role in physical processes once quantum corrections are taken into account. In any event it is clearly of interest to develop and test the predictions based on short-distance perturbation theory as far as possible.

As is well-known, it is the asymptotic freedom,[12,13,14] nature of QCD which allows a perturbative approach to short distance hadronic physics. It is paradoxical that at this time the most important detailed tests of QCD have come from its predictions for scale-breaking corrections to Bjorken scaling for deep inelastic lepton scattering. This is analogous to trying to first verify QED from the radiative correction to a given scattering process, rather than the cross sections itself. However, the most direct test of QCD, to check the form of quark quark or gluon quark scattering at high momentum transfer, at present suffers from a number of experimental and theoretical complications (see Chapter IV). As we shall argue in Chapter II, the most conclusive evidence that the basic Born structure of the theory is correct comes at present from high momentum transfer exclusive processes, particular form factors.

A striking feature of the rigorous QCD operator product analysis of scale breaking effects in deep inelastic processes is the fact that the asymptotic predictions for the q^2 variation of moments, etc. are independent of the nature of target, whether it is a quark, gluon, meson, proton, or nucleus. Although these results are very powerful, they are strictly true only for $q^2 \to \infty$, and the question of non-asymptotic corrections, as well as the nature of the hadronic distribution functions themselves is left unanswered.

In these lectures we shall consider the "synthesis" problem - matching on the QCD scale-breaking form to the hadronic wavefunctions. The analysis given here is based on a collaboration with G. Peter Lepage. Among the questions we shall consider are

(1) What can be predicted for QCD for the form of the structure functions; i.e., what controls the "initial" distributions?
(2) What is the origin of the sea and gluon distribution in QCD?
(3) What are the corrections to the naive probabilistic treatment of the hadron as a classical distribution of the on-shell quarks?
(4) What is the physics and role of higher "twist" operators?

References

1. Yu. L. Dokshitser, D. I. D'yakanov and S. I. Troyan, SLAC-TRANS-183, translations for Proceedings of the 13th Leningrad Winter School on Elementary Particle Physics (1978).

2. C. H. Llewellyn Smith, Oxford preprint 47/48, Lectures presented at the XVII Internationale Universitatswochen für Kernphysik, Schmalding, Austria (1978), published in Acta Physica Austriaca, Suppl. XIX, 331-397 (1978).

3. J. Ellis, SLAC-PUB-2121 (1978); and Proceedings of the SLAC Summer Institute on Particle Physics (1978).

4. C. T. Sachrajda, CERN-TH-2492 (1978); presented at the XIII Rencontre de Moriond.

5. H. Politzer, Phys. Reports 14C (1974).

6. W. Marciano and H. Pagels, Phys. Reports 36C (1978).

7. H. Fritzsch, M. Gell-Mann and H. Leutwyler, Phys. Lett. B47, 365 (1973). For other references, see Refs. 5 and 6.

8. O. W. Greenberg, Phys. Rev. Lett. 13, 598 (1967).

9. P. Cvitanovic, Phys. Rev. D14, 1536 (1976), and references therein.

10. N. Andrei and D. J. Gross, Phys. Rev. D18, 468 (1978); R. D. Carlitz and C. Lee, Phys. Rev. D17, 3238 (1978); L. Baulieu, J. Ellis, M. K. Gaillard and W. J. Zakrzewski, Phys. Lett. 81B, 41 (1979) and 77B, 290 (1978); and T. Appelquist and R. Shankar, Phys. Rev. D18, 2952 (1978).

11. E. Witten, Harvard preprint HUTP-78/A058 (1978).

12. H. Politzer, Phys. Rev. Lett. 30, 1346 (1973).

13. D. J. Gross and F. Wilczek, Phys. Rev. Lett. 30, 1343 (1973).

14. A physical discussion of asymptotic freedom is given by V. F. Weisskopf, Proceedings of the Erice Summer School, Erice Subnucl. Phys. 1974; and R. Field, this volume. An early calculation was given by I. B. Khriplovich, Yad. Fiz. 10, 409 (1969).

15. J. L. Richardson, SLAC-PUB-2229 (1978). See also W. Celmester and F. S. Henyey, Phys. Rev. D17, 3268 (1978).

(Chapter II is available as SLAC-PUB-2294.)

III. TWO-PHOTON COLLISIONS AND SHORT-DISTANCE TESTS OF QUANTUM CHROMODYNAMICS

In this chapter I will review the physics of two-photon collisions in $e^{\pm}$ storage rings with emphasis on the predictions of perturbative quantum chromodynamics for high transverse momentum reactions. Because of the remarkable scaling properties predicted by the theory, two-photon collisions may provide one of the cleanest tests of the QCD picture of short distance hadron dynamics. The contrasts between photon-induced and hadron-induced reactions at high transverse momentum are remarkable and illuminating. Most of the work reported here was done in collaboration with T. DeGrand, J. Gunion, and J. H. Weis.[1] After this short survey of two photon collisions we will go on to the more complicated physics of hadron-hadron collisions.

The photon plays a unique role in strong interaction dynamics because of its elementarity and its direct interactions with the hadronic constituents. Although it is well-known that highly virtual photons have asymptotically scale-free interactions with the quark current in QCD, it is perhaps not sufficiently emphasized that the interactions of real on-shell photons also become dominantly point-like in large momentum transfer (short-distance) processes. The predictions by Bjorken and Paschos[2] for deep inelastic Compton scattering, and dimensional counting predictions[3] for exclusive and inclusive processes involving real photons are all based on the existence of direct $\gamma q\bar{q}$ perturbative couplings, and imply the breakdown of the vector meson dominance description[4] of the photon's hadronic interactions at short-distances and large momentum transfer. As a general rule, VMD can only be valid in QCD for low momentum transfer, nearly on-mass-shell processes where perturbation theory in α_s is invalid. Whenever a photon couples to far-off shell quarks (as in $\gamma q \to \gamma q$) the net real and virtual gluon radiative corrections are of order $\alpha_s(p_T^2) \sim O(\log^{-1}(p_T^2/\Lambda^2))$, and the pointlike Born amplitude are expected to dominate in the asymptotic limit.

The production of hadrons in the collisions of two photons should provide an ideal laboratory for testing many features of the photon's hadronic interactions, including its short distance aspects. It is well known that photon-photon inelastic collisions in e^+e^- storage rings become an increasingly important source of hadrons as the center-of-mass energy $\sqrt{s} = 2E_e$ is raised.[5] The dominant part of the cross section for $e^+e^- \to e^+e^-$ + hadrons arises from the annihilation of two nearly on-shell photons emitted at small angles to the beam (see Fig. 1). The resulting cross section increases logarithmically with energy ($m_e^2/s \to 0$,

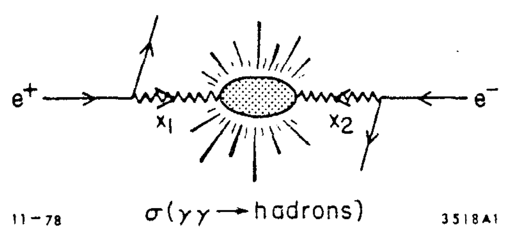

Fig. 1. Two-photon annihilation into hadrons in e^+e^- collisions.

$s \gg m_H^2$):

$$\frac{d\sigma_{e^+e^- \to e^+e^- X}(s)}{dm_H^2} \cong \frac{\alpha^2}{\pi^2} \log^2\left(\frac{s}{m_e^2}\right) \frac{\sigma_{\gamma\gamma}(m_H^2)}{m_H^2} \log\left(\frac{s}{m_H^2}\right) \qquad (1)$$

where m_H is the invariant mass of the produced hadronic system. In contrast, the e^+e^- annihilation cross section decreases quadratically with energy. For example, at the beam energy of $E_e = 15$ GeV, the standard vector dominance estimate for $\sigma_{\gamma\gamma}(m_H^2)$ gives $\sigma(e^+e^- \to e^+e^-$ hadrons) $\cong 15$ nb for $m_H \geq 1$ GeV, compared to the annihilation cross section $\sigma_{e^+e^- \to \gamma \to \text{hadrons}} \equiv R\sigma_{e^+e^- \to \gamma \to \mu^+\mu^-} \cong (0.1\ \text{nb})R$.

The event rate can be large because of (1) the relatively large efficiency for an electron to emit a photon: $(x \equiv (k_0 + k_3)/(p_0 + p_3) \cong \omega/E)$

$$xG_{\gamma/e}(x) = x\frac{dN_{\gamma/e}}{dx} \cong \left(\frac{\alpha}{2\pi} \log\frac{s}{m_e^2}\right)\left(1 + (1-x)^2\right)$$

$$\cong .051 \quad (\sqrt{s} = 30\ \text{GeV},\ x \to 0) \qquad (2)$$

(2) the factor of $\log s/m_H^2$ from the integration over the nearly flat rapidity distribution of the produced hadronic system, and (3) the fact that the cross section is dominated by low-mass hadronic states. For untagged leptons, the cross section for $ee \to eeX$ in the equivalent photon spectrum takes the general form[6]

$$d\sigma_{e^+e^- \to e^+e^- X}(s,t,u) = \int_0^1 dx_1 \int_0^1 dx_2\ G_{\gamma/e}(x_1)\ G_{\gamma/e}(x_2)$$

$$\times\ d\sigma_{\gamma\gamma \to X}\ (\hat{s} = x_1 x_2 s,\ \hat{t} = x_1 t,\ \hat{u} = x_2 u) \qquad (3)$$

where $G_{\gamma/e}(x)$ is the equivalent photon energy spectrum and $d\sigma_{\gamma\gamma \to X}$ is the differential cross section for the scattering of two oppositely directed unpolarized photons (of energy $x_1\sqrt{s}/2$, $x_2\sqrt{s}/2$ in the e^+e^- c.m. system) into a final state X. If the scattered lepton kinematics are measured, then the photon momenta are determined and the full range of hadronic $\gamma\gamma$ physics analogous to pp colliding ring physics becomes accessible.

A large-scale experimental investigation of two-photon physics is now planned at PEP and PETRA. Among the areas of interest are[7]

(a) the production of heavy leptons[8] ($\gamma\gamma \to \tau^+\tau^-$, etc.).
(b) The production of even charge conjugation states and hadronic resonances ($\gamma\gamma \to \eta_c$, etc.).
(c) The measurement of the total $\sigma_{\gamma\gamma}(s)$ cross section, including heavy quark thresholds.
(d) Measurements of the $\pi - \pi$ and $K^+ - K^-$ phase shifts via $\gamma\gamma \to M\bar{M}$ and unitarity, as well as checks of dimensional-coupling scaling laws for the crossed Compton amplitude at large s and t.
(e) Deep inelastic scattering on a photon target,[9] via electrons or positrons tagged at large momentum transfer $e\gamma \to e'X$.

In each case the spacelike mass of each photon can be individually tuned by tagging the scattered $e^\pm$. The photon linear polarization is determined by the lepton scattering plane. We also note that the $e^\pm$ circular polarization of an incident lepton is transferred to the emitted photon with 100% efficiency as $x_\gamma \to 1$.

A. Large p_T Two Photon Reactions

Perhaps the most interesting application of two photon physics is the production of hadrons and hadronic jets at large p_T. The elementary reaction $\gamma\gamma \to q\bar{q} \to$hadrons yields an asymptotically scale-invariant two-jet cross section at large p_T proportional to the fourth power of the quark charge. The $\gamma\gamma \to q\bar{q}$ subprocess[10] implies the production of two non-colinear, roughly coplanar high p_T (SPEAR-like) jets, with a cross section nearly flat in rapidity. Such "short jets" will be readily distinguishable from $e^+e^- \to q\bar{q}$ events due to missing visible energy, even without tagging the forward leptons. It is most useful to determine the ratio,

$$R_{\gamma\gamma} \equiv \frac{d\sigma(e^+e^- \to e^+e^-q\bar{q} \to e^+e^- + \text{jets})}{d\sigma(e^+e^- \to e^+e^-\mu^+\mu^-)} \tag{4}$$

since experimental uncertainties due to tagging efficiency and the equivalent photon approximation tend to cancel. In QCD, with 3-colors, one predicts[1]

$$R_{\gamma\gamma} = 3 \sum_{q=u,d,s,c,\ldots} e_q^4 \left(1 + O\left[\frac{\alpha_s(4p_T^2)}{\pi}\right]\right) \tag{5}$$

where p_T is the total transverse momentum of the jet (or muon) and $\alpha_s(Q^2) \to 4\pi/(\beta \log Q^2/\Lambda^2)$, $\beta = 11-2/3\, n_f$ for n_f flavors. Measurements of the two-jet cross section and $R_{\gamma\gamma}$ will directly test the scaling of the quark propagator $\not{p}^{-1}$ at large momentum transfer, check the color factor[11] and the quark fractional charge. The QCD radiative corrections are expected to depend on the jet production angle and acceptance. Such corrections are of order $\alpha_s(p_T^2)$ since there are neither infrared singularities in the inclusive cross section, nor quark mass singularities at large p_T to give compensating logarithmic factors. The onset of charm and other quark thresholds can be studied once again from the perspective of $\gamma\gamma$-induced processes. The cross section for the production of jets with total hadronic transverse momentum ($p_T > p_{Tmin}$) from the $\gamma\gamma \to q\bar{q}$ subprocess alone can be estimated from the convenient formula,[1,12]

$$\sigma_{e^+e^- \to e^+e^- \mathrm{Jet} + X}(s, p_T^{jet} > p_T^{min}) \equiv R_{\gamma\gamma}\,\sigma_{e^+e^- \to e^+e^-\mu^\pm\mu^\mp}(s, p_T^{\mu\pm} > p_T^{min})$$

$$\cong R_{\gamma\gamma}\,\frac{32\pi\alpha^2}{3}\left(\frac{\alpha}{2\pi}\log\frac{s}{m_e^2}\right)^2 \frac{\left(\log\frac{s}{p_{Tmin}^2} - \frac{19}{6}\right)}{p_{Tmin}^2}$$

$$\cong \frac{0.5\ \mathrm{nb\ GeV}^2}{p_{Tmin}^2} \quad \text{at} \quad \sqrt{s} = 30\ \mathrm{GeV} \quad . \tag{6}$$

where we have taken $R_{\gamma\gamma} = 3\sum_q e_q^4 = 34/27$ above the charm threshold. For $p_{Tmin} = 4$ GeV, $\sqrt{s} = 30$ GeV, this is equivalent to 0.3 of unit of R; i.e., 0.3 times the $e^+e^- \to \mu^+\mu^-$ rate. We note that at $\sqrt{s} = 200$ GeV, the cross section from the $e^+e^- \to e^+e^- q\bar{q}$ subprocess with $p_{Tmin} = 10$ GeV is 0.02 nb, i.e., about 9 units of R! At such energies e^+e^- colliding beam machines are more nearly laboratories for $\gamma\gamma$ scattering then they are for e^+e^- annihilation! A useful graph[12] of the increase in R from the $\gamma\gamma \to q\bar{q}$ process for various $x_{Tmin} = 2p_{Tmin}/\sqrt{s}$ is shown in Fig. 2. The $\log s/p_{Tmin}^2 - 19/6$ in Eq. (6) arises from integration over the nearly flat rapidity distribution of the $\gamma\gamma$ system. The final state in high p_T $\gamma\gamma \to q\bar{q}$ events in the $\gamma\gamma$ center of mass should be very similar in

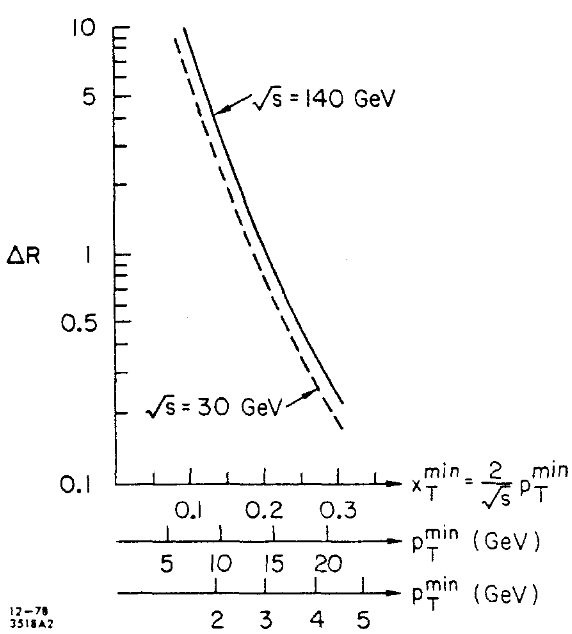

Fig. 2. The contribution to R from $\gamma\gamma \to q\bar{q}$ two jet processes at $\sqrt{s} = 30$ and 140 GeV (from Ref. 12).

multiplicity and other hadronic properties as $e^+e^- \to \gamma^* \to q\bar{q}$, although $u\bar{u}$ and $c\bar{c}$ events should be enhanced relative to $d\bar{d}$ and $s\bar{s}$ due to the e_q^4 dependence. Monte Carlo studies of SPEAR events at $s = 4p_T^2$ distributed uniformly in rapidity would be useful in order to learn how to identify and trigger $\gamma\gamma \to q\bar{q}$ events.

Although the above prediction for $R_{\gamma\gamma}$ is one of the most straightforward consequences of perturbative QCD, it should be noted that from the perspective of photon physics of 10 years ago, the occurence of events with the structure $\gamma\gamma \to \text{jet} + \text{jet}$ at high p_T could only be regarded as revolutionary. From the VMD standpoint, a real photon acts essentially as a sum of vector mesons; however, it is difficult to imagine an inelastic collision of two hadrons producing two large p_T jets without energy remaining in the beam direction!

On the other hand, if the $\gamma\gamma \to$ two jet events are not seen at close to the predicted magnitude with an approximately scale invariant cross section, then it would be hard to understand how the perturbative structure of QCD could be applicable to hadronic physics. In particular, unless the pointlike couplings of real photons to quarks are confirmed, then the analogous predictions for perturbative high p_T processes, involving gluons such as $gg \to q\bar{q}$ are probably meaningless.

B. Multi-Jet Processes and the Photon Structure Function

In addition to the two-jet processes, QCD also predicts 3- and 4-jet events from subprocesses such as $\gamma q \to gq$ (3-jet production where one photon interacts with the quark constituent of the other photon) as well as the conventional high p_T QCD subprocesses $qq \to qq$ and $q\bar{q} \to gg$ (which lead to jets down the beam direction plus jets at large p_T) (see Fig. 3). The structure of these events are very similar to that for hadron-hadron collisions. The cross section for $E d\sigma/d^3p_J$ ($\gamma\gamma \to \text{jet} + X$ or $ee \to ee\ \text{jet} + X$) can be computed in the standard way from the hard scattering expansion ($\hat{s} = x_a x_b s$, etc.)[13]

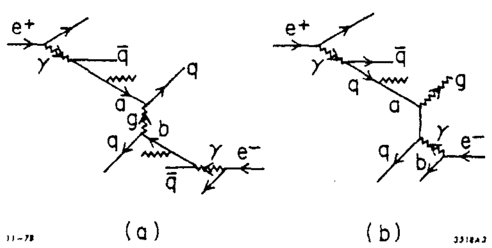

Fig. 3. Contributions from QCD subprocesses to (a) 4-jet and (b) 3-jet final states.

$$E \frac{d\sigma}{d^3p}(AB \to CX) = \sum_{abd} \int_0^1 dx_a \int_0^1 dx_b\ G_{a/A}(x_a)\ G_{b/B}(x_b)$$

$$\frac{d\sigma}{d\hat{t}}(ab \to cd)\Big|_{s,t,u} \frac{\hat{s}}{\pi}\, \delta(\hat{s} + \hat{t} + \hat{u}) \qquad (7)$$

where the hard scattering occurs in $ab \to cd$ and the fragmentation function $G_{a/A}(x_a)$ gives the probability of finding constituent a with light-cone fraction $x_a = (p_a^0 + p_a^3)/(p_A^0 + p_A^3)$. In general, $G_{a/A}$ has a scale-breaking dependence on log p_T^2 which arises from the constituent transverse momentum integration when gluon bremsstrahlung or pair production is involved.[14]

However, there is an extraordinary difference between photon and hadron induced processes. In the case of proton-induced reactions, $G_{q/p}(x,Q^2)$ is determined from experiment, especially deep inelastic lepton scattering. In the case of the photon, the $G_{q/\gamma}$ structure function required in Eq. (7) has a perturbative component which can be predicted from first principles in QCD. This component, as first computed by Witten,[15] has the asymptotic form at large probe momentum Q^2

$$G_{q/\gamma}(x,Q^2) \implies \frac{\alpha}{\alpha_s(Q^2)} f(x) + O(\alpha^2) \tag{8}$$

i.e.: aside from an overall logarithmic factor, the $\gamma \to q$ distribution Bjorken scales; $f(x)$ is a known, calculable function. Unlike the proton structure function which contracts to $x = 0$ at infinite probe momentum $Q^2 \to \infty$, this component of the photon structure function increases as log Q^2 independent of x. This striking fact is of course due to the direct $\gamma \to q\bar{q}$ perturbative component in the photon wavefunction. (The apparent violation of momentum conservation when $\alpha_s(Q^2) < \alpha$ should be cured when higher order terms in α are taken into account.) In addition to the perturbative component, one also expects a nominal hadronic component due to intermediate vector meson states.

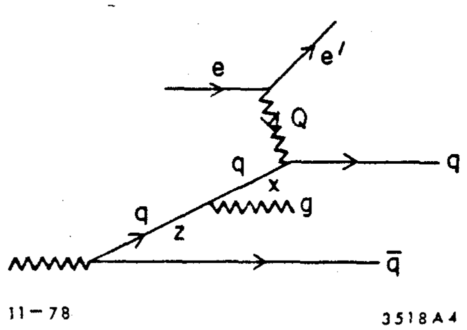

Fig. 4. Representation of the QCD photon structure function in deep inelastic scattering on a photon target. Real and virtual gluon corrections to all orders are included in the analytic results.

The calculation of the photon structure function is straightforward if we keep only leading logarithms in each order of perturbation theory. The leading contribution can be written as a simple convolution: (see Fig. 4)[14]

$$G_{q/\gamma}(x,Q^2) = \frac{3\alpha}{2\pi} e_q^2 \int_{\mu^2}^{Q^2} \frac{dk^2}{k^2} \int_x^1 \frac{dz}{z} \left[z^2 + (1-z)^2\right] G_{q/q}\left(\frac{x}{z}, Q^2, k^2\right) \tag{9}$$

where $G_{q/q}(x/z,Q^2,k^2)$ is the standard non-singlet distribution due to gluon bremsstrahlung for quarks in a target quark of mass k^2 being probed at four-momentum squared Q^2. The factor of three includes the sum over quark colors. In addition one can include smaller sea quark contributions form $g \to q\bar{q}$ processes. The region $k^2 < \mu^2$ can be identified with the VDM contribution to $G_{q/\gamma}$.

Taking moments, we have[1]

$$G_{q/\gamma}(j,Q^2) = \frac{3\alpha}{2\pi} e_q^2 \int_{\mu^2}^{Q^2} \frac{dk^2}{k^2} f(j)\, G_{q/q}(j,Q^2,k^2) \tag{10}$$

where

$$G(j) \equiv \int_0^1 dx\, x^{j-1}\, G(x) \tag{11}$$

$$f(j) = \int_0^1 dz\, z^{j-1} \left(z^2 + (1-z)^2 \right)$$

$$= \frac{1}{j} - \frac{2}{j+1} + \frac{2}{j+2} \tag{12}$$

and

$$G_{q/q}(j,Q^2,k^2) = \left[\frac{\alpha_s(k^2)}{\alpha_s(Q^2)} \right]^{\gamma_{j-1}} \tag{13}$$

The γ_j are the standard valence anomalous dimensions, as defined in (II.2.18). Performing the k^2 integral in (10) yields

$$G_{q/\gamma}(j,Q^2) = \frac{3}{2\pi} e_q^2 \frac{\alpha}{\alpha_s(Q^2)} \left[\frac{4\pi f(j)}{\beta(1-\gamma_{j-1})} \right] \tag{14}$$

This exhibits the remarkable scaling features of the photon structure function discussed above.

It is easy to invert the moment equation via the method of Yndurian.[16] A graph of $xG_{q/\gamma}(x)$ calculated in valence approximation in QCD and in the parton model is given in Fig. 5. Good agreement is obtained with the (valence plus singlet) results of Llewellyn Smith[5] over nearly the entire range of x.

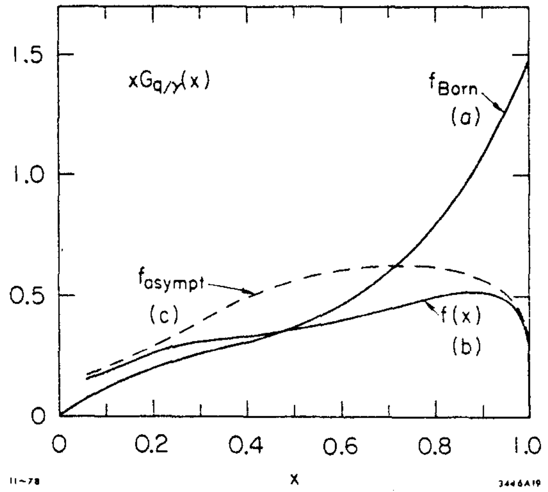

Fig. 5. The valence photon structure function $G_{q/\gamma}(x)$ as calculated in (a) Born approximation, (b) to all orders in QCD, and (c) the $x \to 1$ limit (Eq. (17)). An overall factor proportional to $\log Q^2/\Lambda^2$ is factored out (from Ref. 1).

The x near 1 behavior of $G_{q/\gamma}(x)$ can be obtained more directly from a direct integration of (10), using the $x \to 1$ form for the quark structure function[14]

$$G_{q/q}(x,Q^2,k^2) = \frac{\exp\left[(3-4\gamma_E)\xi C_2\right](1-x)^{4C_2\xi-1}}{\Gamma(4C_2\xi)} \tag{15}$$

where $\gamma_E = 0.577\ldots$ is Euler's constant, $C_2 = (N^2-1)/2N = 4/3$, and

$$\xi = \frac{1}{\beta} \ln \frac{\alpha_s(k^2)}{\alpha_s(Q^2)} \tag{16}$$

One then obtains[14]

$$G_{q/\gamma}(x,Q^2) \underset{x\to 1}{=} \frac{3}{2\pi} e_Q^2 \frac{\alpha}{\alpha_s(Q^2)} \quad \frac{4}{\beta - (3-4\gamma_E)C_2 + 4C_2 \ln\frac{1}{1-x}} \tag{17}$$

This result is numerically accurate only for $x \gtrsim 0.97$ but is off by no more than a factor of 2 for $x > 0.1$ (see Fig. 5).

It is interesting to note that for fixed $\mathcal{M}^2$, $Q^2 \to \infty$, this expression for $G_{q/\gamma}(x,Q^2)$ approaches a constant. This implies, via the Drell-Yan relation, perfect power-law scaling for the $\gamma \to \pi^0$ transition form factor. [See Eq. (2.26), Chapter II.]

Compared to meson distributions which fall as a power at $x \to 1$, the photon structure function is nearly flat in x, again due to the underlying $\gamma q\bar{q}$ pointlike vertex. In principle the photon structure can be determined experimentally from the two photon $e\gamma \to e'X$ process, i.e.; deep inelastic scattering from a photon target.[9]

Returning to the high p_T jet cross sections, we note the following striking fact: in each contribution to the four-jet cross section the two factors of $\alpha_s(p_T^2)$ from the subprocess cross section, e.g.,

$$\frac{d\sigma}{dt}\,(qq \to qq) \sim \frac{2}{9}\,\frac{4\pi\alpha_s^2(t)}{t^2} \tag{18}$$

(see Fig. 3a) actually cancel (in the asymptotic limit) the two inverse powers of $\alpha_s(p_T^2)$ from the two $G_{q/\gamma}(x,p_T^2)$ structure functions.[1] Similarly the single power of $\alpha_s(p_T^2)$ in $d\sigma/dt\;(\gamma q \to gq)$ cancels the single inverse power of $\alpha_s(p_T^2)$ structure function in the 3-jet cross section. (See Fig. 3b.) Thus miraculously all of these jet trigger cross sections obey exact Bjorken scaling

$$E\,\frac{d\sigma}{d^3p}\,(\gamma\gamma \to \mathrm{Jet} + X) \underset{p_T^2 \to \infty}{\Longrightarrow} \frac{1}{p_T^4}\, f(x_T\,,\, \theta_{cm}) \tag{19}$$

when the leading QCD perturbative corrections to all orders are taken into account.[17] Furthermore, the asymptotic cross sections are even independent of $\alpha_s(p_T^2)$! The asymptotic prediction thus has essentially zero parameters.

Quite detailed numerical predictions can be made for the $ee \to ee$ Jet + X cross sections by computing $G_{q/e}$ (from the convolution of the equivalent photon approximation $G_{\gamma/e}$ and the photon structure function $G_{q/\gamma}$), and then summing in Eq. (7) over all 2-2 hard scattering QCD processes, including all quark colors and flavors. In our calculations[1] we have found it useful to display approximate analytic forms which have the correct power-law dependence at large p_T and at the edge of phase space ($x_R = 2p_J/\sqrt{s} \to 1$). The analytic forms usually agree with the numerically integrated results to within 20%. For the analytic calculations, we have used the simplified form

$$xG_{q/e}(x) = e_q^2\left(\frac{\alpha}{2\pi}\log\eta\right)\frac{\alpha}{2\pi}\,F_Q(1-x) \tag{20}$$

for each quark flavor and color, where $\log\eta = \log s/4m_e^2$ if the scattered electron is not tagged. The factor F_Q which is $\sim \log s/4m_q^2$ if we use the Born approximation for $\gamma \to q\bar{q}$, becomes of order $1/\alpha_s\,(Q^2)$ when the QCD radiative corrections are taken into account. We have found empirically that the value $\alpha_s(Q^2)F_Q \cong 0.8$ gives a good characterization of the QCD normalization. [For $x \to 1$ $G_{q/e}$ actually falls as $(1-x)\,\log 1/(1-x)$.] Note also that for $x \to 1$, the quark and electron tend to have the same helicity.

For the 4-jet cross section, the sum over all types of jet triggers near 90° gives

$$E\,\frac{d\sigma}{d^3p_J}\,(e^+e^-\to e^+e^-\,\mathrm{Jet}+X) \cong \left(\frac{\alpha}{2\pi}\log\eta\right)^2 \left[\frac{\alpha}{2\pi}F_Q\,\alpha_s(p_T^2)\right]^2$$

$$\cdot\left[80\left(\sum_f e_f^2\right)^2 + \frac{52}{9}\left(\sum_f e_f^4\right)\right]\frac{(1-x_R)^3}{p_T^4}$$

$$= \quad 0.8\times 10^{-2}\ \mathrm{nb\ GeV}^2\ \frac{(1-x_R)^3}{p_T^4}\quad [\sqrt{s}=30\ \mathrm{GeV}]. \qquad (21)$$

The sum f is over contributing quark flavors. The subprocesses include $qq\to qq$, $q\bar{q}\to q\bar{q}$, and $q\bar{q}\to gg$.

For the 3-jet events, the subporcesses $\gamma q\to gq$ and $\gamma\bar{q}\to g\bar{q}$ yield the cross section

$$E\,\frac{d\sigma}{d^3p_J}\,(e^+e^-\to e^+e^-\,\mathrm{Jet}+X) \cong \alpha\left(\frac{\alpha}{2\pi}\log\eta\right)^2 \left[\frac{\alpha}{2\pi}F_Q\,\alpha_s(p_T^2)\right]$$

$$\cdot\left[40\sum_f e_q^4\right]\frac{(1-x_R)^2}{p_T^4}$$

$$\cong \quad 2.5\times 10^{-2}\ \mathrm{nb\ GeV}^2\ \frac{(1-x_R)^2}{p_T^4}\quad [\sqrt{s}=30\ \mathrm{GeV}]. \qquad (22)$$

The corresponding result for the two jet cross section from $\gamma\gamma\to q\bar{q}$ is

$$E\,\frac{d\sigma}{d^3p_J}\,(e^+e^-\to e^+e^-\,\mathrm{Jet}+X) \cong 3\times 10^{-2}\ \mathrm{nb\ GeV}^2\ \frac{(1-x_R)}{p_T^4}\,, \qquad (23)$$

i.e.: in general, $\sigma(2\ \mathrm{jet}) > \sigma(3\ \mathrm{jet}) > \sigma(4\ \mathrm{jet})$. It is clear that there is no double counting of cross sections here since each type of jet cross section has a distinctive topological structure and different pattern of q, $\bar{q}$ and g jets. A graph of these cross sections is shown in Fig. 6.

To remind ourselves how critical the pointlike photon couplings are to these results, let us estimate the contribution to high p_T jet production when both photons are meson dominated. We have

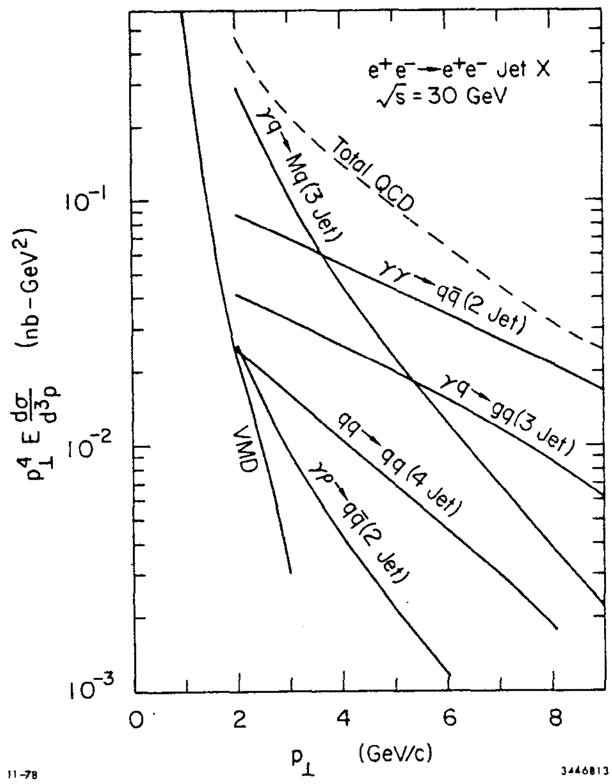

Fig. 6. QCD (and VMD) contributions to the $e^+e^- \to e^+e^-$ Jet + X. The 4-jet cross section includes the contributions from $qq \to qq$, $q\bar{q} \to q\bar{q}$, and $q\bar{q} \to gg$ (from Ref. 1).

$(f_\rho^2/4\pi \cong 2)$

$$d\sigma^{VDM} \, (\gamma\gamma \to Jet + X)$$

$$= \left(\frac{e}{f_\rho}\right)^4 d\sigma \; (\rho\rho \to Jet + X)$$

$$\cong \left(\frac{4\pi\alpha}{f_\rho^2}\right)^2 \left(\frac{2}{3}\right)^2$$

$$\times \; \frac{d\sigma(pp \to Jet + X)}{(1-x_R)^4} \qquad (24)$$

since we expect $G_{q/p} \sim (1-x)^2 G_{q/\rho}$. If we take $E d\sigma \; (pp \to Jet + X)/d^3p \sim 300 \times E d\sigma/d^3p \; (pp \to \pi X) \sim 1.1 \text{ nb GeV}^6 \; (1-x_R)^9 \; p_T^{-8}$, then the convolution over photon momentum distributions yields the rough estimate ($\theta_{cm} \cong 90^\circ$, $\sqrt{s} = 30$ GeV):

$$E \frac{d\sigma^{VDM}}{d^3p_J} \, (e^+e^- \to e^+e^- \; Jet + X) \;\; \cong \;\; 1.4 \text{ nb GeV}^6 \; \frac{(1-x_R)^7}{p_T^4} \;, \qquad (25)$$

which is negligible compared to the pointlike contributions for $p_T > 2$ GeV (see Fig. 6). We have also checked explicitly that the QCD ($q\bar{q} \to q\bar{q}$ hard scattering) contributions from processes such as $\gamma\rho \to q\bar{q}q\bar{q}$ or $\rho\rho \to q\bar{q}q\bar{q}$, where one or both photons are meson dominated, are also small.

The overall scaling properties of QCD cross sections due to specific subprocesses can be easily determined from counting rules:[18]

$$E \frac{d\sigma}{d^3p} \, (A+B \to C+X) \;\; \cong \;\; \frac{f(\theta_{cm})}{(p_T^2)^{n_{active} - 2}} \, (1-x_R)^{2n_{spect}^{bnd} + n_{fm} - 1} \qquad (26)$$

where n_{active} is the number of elementary fields (q,e,γ,g, etc.) participating in the hard scattering subprocess,[3] n^{bnd}_{spect} is the number of bound spectators, i.e.: the number of constituent fields which do not interact (and thus "waste" the incident energy),[19] and n_{fm} are the number of unbound spectator fermions (q,e) from pair production or bremsstrahlung scattering processes, as in the equivalent photon approximation. In Eqs. (21)-(23) the number of active fields in each case is 4; $n^{bnd}_{spect} = 0$, and $n_{fm} = 4,3$, and 2 respectively. The counting rules have small corrections due to logarithmic scale-breaking effects and the log (1/1-x) behavior of $G_{q/\gamma}$.

C. High p_T Meson Production in γγ and pp Collisions

We have also considered in some detail background contributions to the $\gamma q \to \text{Jet} + X$ cross section from (higher "twist") subprocesses that involve more than the minimum number of active fields in the hard scattering subprocess.[20] The most significant background comes from subprocesses of the form (see Fig. 7)

$$\gamma q \to Mq$$

where a photon from one beam photoproduces a meson at large p_T on a quark constituent of the other beam. The meson trigger, the recoil quark jet, and the spectator $\bar{q}$ jet together provides a background to the $\gamma\gamma \to$ 3-jet events.

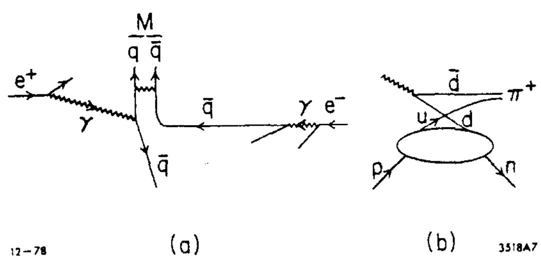

Fig. 7. Contribution of the $\gamma q \to Mq$ subprocesses to (a) $e^+e^- \to e^+e^-\pi^+X$ and (b) $\gamma p \to \pi^+ n$.

The normalization of the $\gamma q \to Mq$ amplitude can be inferred in a straightforward way from $\gamma p \to \pi^+ n$ photoproduction at large momentum transfer: (see Fig. 7(b))

$$\frac{d\sigma}{dt}(\gamma p \to \pi^+ n) \propto F_p^2(t)\, \frac{d\hat{\sigma}}{dt}(\gamma q \to \pi q) \tag{27}$$

The 90° exclusive cross section[21] falls as $s^{-7.3 \pm 0.4}$ in agreement with the s^{-7} behavior predicted by Eq. (27), and dimensional counting.[3] [See Chapter II.] The net result is

$$(n_{active} = 5)\quad E\frac{d\sigma}{d^3p}(e^+e^- \to e^+e^-\ \text{Jet} + X) = 1.1\ \text{nb GeV}^4\ (1-x_R)^2/p_T^6$$

where the sum over all pseudo-scalar and vector meson $q\bar{q}$ bound states in the $\underline{35}+\underline{1}$ representation of SU(3) constitutes the "jet" trigger. As shown in Fig. 6, this contribution falls faster in p_T but at $\sqrt{s} = 30$ GeV dominates the $\gamma q \to gq$ 3-jet cross section until $p_T^{jet} \sim$ 6 GeV, and (though distinguishable by topology) it even dominantes the $\gamma\gamma \to q\bar{q}$ contribution until $p_T^{jet} \gtrsim 4$ GeV.

It is possible that the normalization of the $\gamma q \to Mq$ subprocess has been overestimated; nevertheless this amplitude must occur at some level, producing a characteristic $p_T^{-6}\ f(x_R, \theta_{cm})$ cross section. The most important check of its contribution will come from single particle production at large p_T, such as $e^+e^- \to e^+e^-\pi^+X$. In the case of hard scattering processes such as $\gamma\gamma \to q\bar{q}$, $\gamma q \to gq$, and $qq \to qq$, the final state fragmentation $G_{\pi/q} \sim (1-x)$ leads to a strong suppression ($\sim 10^{-2}$) in the π^+/Jet ratio, since the quark jet must be produced at higher momentum than the trigger particle (the "trigger bias" effect).[22] For example, the leading $\gamma\gamma \to q\bar{q}$ subprocess gives

$$E\frac{d\sigma}{d^3p}\,(e^+e^- \to e^+e^-\pi^+X) = 6\times 10^{-4}\ \text{nb GeV}^2\ \frac{(1-x_R)^3}{p_T^4}\ . \tag{28}$$

On the other hand, the $\gamma q \to \pi^+ q$ subprocess produces a pion at high p_T, without suppression from fragmentation:

$$E\frac{d\sigma}{d^3p}\,(e^+e^- \to e^+e^-\pi^+_{\text{prompt}}X) = 3\times 10^{-2}\ \text{nb GeV}^2\ \frac{(1-x_R)^2}{p_T^6}\ . \tag{29}$$

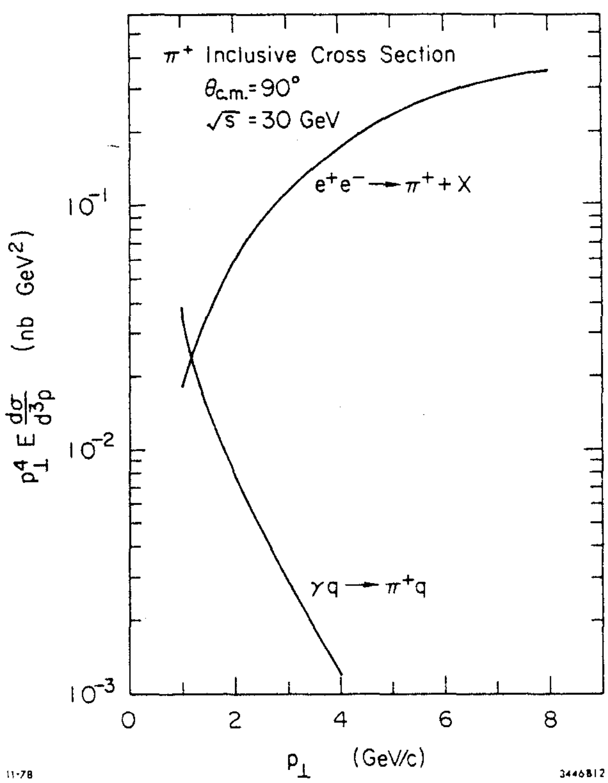

Fig. 8. Leading contributions to inclusive pion contributions from e^+e^- annihilation and $e^+e^- \to e^+e^-\pi^+X$ (from Ref. 1).

(Inclusion of non-"prompt" π's from resonance decay approximately doubles the production rate.) This contribution is thus predicted to dominate single pion production in the $\gamma\gamma$ process until very high p_T. With the above normalization, and in the absence of electron or positron tagging, the two-photon reaction provides a significant background to the 90° inclusive π^+ spectrum from $e^+e^- \to \gamma^* \to \pi^+ + X$ for $x_T \lesssim 0.15$ at $\sqrt{s} = 30$ GeV. (See Fig. 8.)

It will be extremely interesting to verify the normalization and especially the power law of the $\gamma\gamma \to \pi^+ + X$ cross section. The p_T^{-6} power is derived directly from the lowest order diagram for $\gamma q \to (q\bar{q})q$ where the $q\bar{q}$ system is at fixed mass; higher order QCD corrections can only modify the result by an overall logarithmic factor. The fact that the single hadron trigger is produced directly in the hard scattering subprocess rather than by quark or gluon fragmentation also is an important feature in hadron-hadron collision. In this case, as described in the constituent interchange model (CIM),[20] dominant subprocess contributing to the $pp \to \pi^+ X$ and $pp \to pX$ cross sections for $p_T < 8$ GeV are expected to be the prompt hard-scattering reactions such as $qM \to qM$ and $qB \to qB$, respectively. These subprocesses immediately explain why the observed power law for $Ed\sigma/d^3p$ at fixed x_T and θ_{cm} are close to p_T^{-8} (meson production) and p_T^{-12} (proton production) for data below $p_T = 8$ GeV. The CIM approach also can account for the observed angular distributions, same side momentum correlations, and charge correlations (flavor transfer) between opposite sides.[23] We will discuss the central issues for hadron collisions in the next chapter.

In summary, it becomes evident that two photon collisions can provide a clean and elegant testing ground for perturbative quantum chromodynamics. The occurrence of $\gamma\gamma$ reactions at an experimentally observable level implies that the entire range of hadronic physics which can be studied, for example, at the CERN-ISR can also be studied in parallel in $e^\pm e^-$ machines. Although low p_T $\gamma\gamma$ reactions should strongly resemble meson-meson collisions, the elementary field nature of the photon implies dramatic differences at large p_T. We have especially noted the sharp contrasts between hadron-and photon-induced reactions due to the photon's pointlike coupling to the quark current and the ability of a photon to give nearly all of its momentum to a quark. The large momentum transfer region can be a crucial testing ground for QCD since not only are a number of new subprocesses accessible ($\gamma\gamma \to q\bar{q}$, $\gamma q \to gq$, $\gamma q \to Mq$, deep inelastic scattering on a photon target) with essentially with no free parameters, but most important, one can make predictions for a major component of the photon structure function directly from QCD. We also note that there are open questions in hadron-hadron collisions, e.g., whether non-perturbative effects (instantons, wee parton interactions) are important for large p_T reactions.[24] Such effects are presumably absent for the perturbative, pointlike interactions of the photon. We also note that the interplay between vector-meson-dominance and pointlike contributions to the hadronic interactions of photon is not completely understood in QCD, and $\gamma\gamma$ processes may illuminate these questions.

Footnotes and References

1. S. J. Brodsky, T. A. DeGrand, J. F. Gunion and J. H. Weis, Phys. Rev. Lett. 41, 672 (1978); and SLAC-PUB-2199 (submitted to Phys. Rev.).

2. J. D. Bjorken and E. A. Paschos, Phys. Rev. 185, 1975 (1969).

3. S. J. Brodsky and G. Farrar, Phys. Rev. Lett. 31, 1153 (1973); Phys. Rev. D11, 1309 (1975); V. A. Matveev, R. M. Muradyan and A. N. Tavkheldize, Lett. Nuovo Cimento 7, 719 (1973).

4. For a comprehensive review of the vector meson dominance model, see T. H. Bauer, R. D. Spital, F. M. Pipkin and D. R. Yennie, Rev. Mod. Phys. 50, 261 (1978).

5. S. J. Brodsky, T. Kinoshita and H. Terazawa, Phys. Rev. D4, 1532 (1971). For reviews see V. M. Budnev *et al.*, Phys. Reports 15C (1975); H. Terazawa, Rev. Mod. Phys. 45, 615 (1973); and the reports of S. J. Brodsky, H. Terazawa and T. Walsh in the Proceedings of the International Colloquium on Photon-Photon Collisions, published in Supplement au Journal de Physique, Vol. 35 (1974). See also, G. Grammer and T. Kinoshita, Nucl. Phys. B80, 461 (1974); R. Bhattacharya, J. Smith and G. Grammer, Phys. Rev. D15, 3267 (1977); J. Smith, J. Vermaseren and G. Grammer, Phys. Rev. D15, 3280 (1977).

6. See S. J. Brodsky *et al.*, Ref. 5, and F. Low, Phys. Rev. 120, 582 (1960). In the case of tagged leptons log $s/m_e^2 \to \sim\log \theta^2_{max}/\theta^2_{min}$. Derivations and more precise formula are given in Ref. 5. An excellent discussion of the experimental considerations is given by J. Field, LEP Summer Study/1-13, October 1978.

7. For discussion and references, see S. J. Brodsky, Ref. 5.

8. For detailed calculations see J. Smith *et al.*, Ref. 5, and J. Field, Ref. 6. The $e^+e^- \to e^+e^-\tau^+\tau^-$ cross section is comparable to the $e^+e^- \to \tau^+\tau^-$ cross section at $\sqrt{s} = 30$ GeV.

9. S. J. Brodsky, T. Kinoshita and H. Terazawa, Phys. Rev. Lett. 27, 280 (1971); T. F. Walsh, Phys. Lett. 36B, 121 (1971).

10. The $\gamma\gamma \to q\bar{q}$ process for single hadron production at large p_T in e^+e^- collisions was first considered in the pioneering paper by J. D. Bjorken, S. Berman and J. Kogut, Phys. Rev. D4, 3388 (1971). A discussion of this process for virtual γ reactions has been given by T. F. Walsh and P. Zerwas, Phys. Lett. 44B, 195 (1973).

11. In the case of integrally-charged Han-Nambu quarks, locality of the $\gamma\gamma \to q\bar{q}$ matrix element at high p_T implies for the u,d first generation quarks

$$\mathcal{M}_{\gamma\gamma} \propto \langle 0 | j^2_{em}(0) | X \rangle = \begin{cases} \sum\limits_{c=R,Y,B} u^\dagger_c u_c \left(\frac{2}{3}\right) + d^\dagger_c d_c \left(\frac{1}{3}\right) & \begin{pmatrix} \text{below} \\ \text{color} \\ \text{threshold} \end{pmatrix} \\ u^\dagger_R u_R + u^\dagger_B u_B + d^\dagger_Y d_Y & \begin{pmatrix} \text{above} \\ \text{color} \\ \text{threshold} \end{pmatrix} \end{cases}$$

which aside from a sign change for the down quark is identical to the $\langle 0 | j_{em}(0) | X \rangle$ matrix element. Thus, we have the identity

$$R^{HN}_{\gamma\gamma} = R$$

both below and above the color threshold. In particular, $R^{HN}_{\gamma\gamma} = 5/3 \times$ (number of flavor generations) below color threshold, and $R^{HN}_{\gamma\gamma} = 3 \times$ (number of flavor generations) above color threshold, compared to $17/27 \times$ (number of flavor generations) for the standard QCD model. See also M. Chanowitz in "Color Symmetry and Quark Confinement," Proceedings of the 12th Rencontre de Moriond, 1977, edited by Tran Thanh Van, and P. V. Landshoff, LEP Summer Study/1-13, October 1978.

12. Equation (6) has also been derived in an equivalent form by K. Kajantie, University of Helsinki reprint, September 1978.

13. For a review see D. Sivers, R. Blankenbecler and S. J. Brodsky, Phys. Reports 23C:1 (1976). For a discussion of the validity of the hard scattering expansion in field theory, see W. E. Caswell, R. R. Horgan and S. J. Brodsky, Phys. Rev. D18, 2415 (1978). Note that processes where one electron balances the transverse moment of the high p_T jet trigger also occur in (3).

14. Yu. L. Dokshitser, D. I. D'Yakanov and S. I. Troyan, Stanford Linear Accelerator Center translation SLAC-TRANS-183, translated for Proceedings of the 13th Leningrad Winter School on Elementary Particle Physics, 1978.

15. E. Witten, Nucl. Phys. B120, 189 (1977). The results of Witten have been rederived by summing ladder graphs by W. Frazer and J. Gunion, University of California at Davis preprint 10P10-194 (1978) and by C. H. Llewellyn Smith, Oxford preprint 67/78. See also Ref. 14.

16. F. J. Yndurian, Phys. Lett. 74B, 68 (1978).

17. This remarkable scaling property was first pointed out by C. H. Llewellyn Smith, Oxford preprint 56/78 (1978).

18. See Refs. 13, R. Blankenbecler, S. J. Brodsky and J. F. Gunion, Phys. Rev. D18, 900 (1978), and Ref. 1. If the spin of a constituent a does not match that of the projectile A, then one expects a suppression factor $(1-x)^{2|S_z^a - S_z^A|}$ in the leading scaling term. S. J. Brodsky, J. F. Gunion and M. Scadron (to be published). Logarithmic QCD corrections to the power-law behavior are discussed in Chapter II.

19. S. J. Brodsky and R. Blankenbecler, Phys. Rev. D10, 2973 (1974).

20. R. Blankenbecler, S. J. Brodsky and J. F. Gunion, Phys. Rev. D18, 900 (1978); P. V. Landshoff and J. C. Polkinghorne, Phys. Rev. D8, 927 (1973), Phys. Rev. D10, 891 (1974).

21. R. Anderson *et al*., Phys. Rev. Lett. 30, 627 (1973). For a comparison of Compton scattering and photoproduction, see M. A. Shupe *et al*., Cornell preprints (1978). [See Chapter II.]

22. S. D. Ellis, M. Jacob and P. V. Landshoff, Nucl. Phys. B108, 93 (1976). See also J. D. Bjorken and G. R. Farrar, Phys. Rev. D9, 1449 (1974).

23. For recent discussions see S. J. Brodsky, SLAC-PUB-2217, October 1978, and D. Jones and J. F. Gunion, Phys. Rev. D9, 1032 (1979). Also see Chapters II and IV.

24. I wish to thank J. Ellis for conversations on this point.

IV. HADRON AND PHOTON PRODUCTION AT LARGE TRANSVERSE MOMENTUM AND THE DYNAMICS OF QCD JETS

1. Introduction

The most direct tests of the interactions of quarks and gluons at short distances involve the production of single hadrons, hadronic jets, and photons at large transverse momentum. In this chapter we will review several areas of hadronic phenomenology which test predictions of quantum chromodynamics calculated from perturbation theory, including:

(a) The production of direct photons at large transverse momentum in hadron-hadron collisions.[1,2] In perturbative QCD, the ratio of gluon jet and direct photon cross sections is directly calculable, and leads to important phenomenological constraints.
(b) The multiplicity and distribution of hadrons in inclusive reactions may be related to color separation of the initiating subprocesses.[3,4] The consequences of this ansatz for gluon and quark jets are discussed. We also review other possible discriminants of jet parentage.
(c) The hadronic decay of the upsilon via three gluon jet[5,6] or a photon plus two gluon jets[6] could provide some of the most definite tests of QCD.
(d) Gluon jets may be "oblate" with principal axes correlated with the gluon polarization.[7]
(e) The gluon distribution of a hadron is connected with the size of the source due to coherent effects and is not determined solely by the quark distribution.[8]

At present, the most controversial area of QCD phenomenology concerns the production of single hadrons at large transverse momentum in proton-proton collisions.[9,10] We shall begin our discussion with a short review of the current issues.

2. Production of Large Transverse Momentum Particles in Hadron-Hadron Collisions

There are currently two main approaches to large p_T phenomena -- both based on perturbative QCD and a "hard scattering expansion."

(A) Quark, gluon scattering models. The basic collision subprocesses responsible for the large momentum transfer are assumed to be $qq \to qq$, $qg \to qg$, and $gg \to gg$, as calculated in Born approximation QCD.[11] Violation of scale-invariance occurs through the running coupling constant $\alpha_s(Q^2)$, the quark and gluon structure functions, and the transverse momentum (k_T) distributions of the constituents in the hadronic wavefunctions. The calculations automatically include those parts of higher particle number subprocesses such as $qq \to qqg$ which contribute to logarithmic scaling violations in the structure functions.

(B) The Constituent Interchange Model.[12] In addition to all of the contributions listed in (A), QCD also predicts "higher twist" subprocesses[13] where more than the minimal number of quark and gluon fields participate in the hard scattering reaction, such as $qM \to qM'$, $qB \to qB'$, $gq \to Mq$, $q\bar{q} \to M\bar{M}$, etc. Here "M" and "B" indicate $q\bar{q}$ and qqq clusters of fixed mass relative to p_T. The cross sections for these subprocesses are readily computed from minimal QCD diagrams.[13,14] As in (A) logarithmic scaling violations occur.[15] By definition, higher twist subprocesses are responsible for all large p_T exclusive reactions involving hadrons.

The basic distinction between these two approaches for an inclusive reaction such as $pp \to \pi X$ is simply whether (a) the high p_T trigger meson is formed after the hard scattering (e.g., $q_1q_2 \to q_1q_2$ with $q_1 \to q_1 + \pi$) or (b) formed before the collision and then scattered (e.g., $\pi q \to \pi q$). Obviously both types of subprocesses contribute to the cross section at some level -- it is a question of kinematics where each dominates: for fixed $x_T = 2p_T/s$ and θ_{cm}, the Born contributions clearly dominate at $p_T \to \infty$ since

$$\frac{\frac{d\sigma}{dt}\,(\pi q \to \pi q)}{\frac{d\sigma}{dt}\,(qq \to qq)} \sim F_\pi^2(p_T^2) \sim O\left[\frac{1\ \mathrm{GeV}^4}{p_T^4}\right] . \qquad (2.1)$$

On the other hand, the necessity for final state fragmentation in any quark or gluon scattering reaction implies a numerical suppression of the cross section by 2 to 3 orders of magnitude! This crucial factor (called "trigger bias" by Ellis, Jacob, and Landshoff[16]) results because a quark typically gives 75% of its momentum to the trigger particle due to its rapidly falling fragmentation function $G_{\pi/q}(z)$ at $z \sim 1$. The $qq \to qq$ subprocess then occurs at an effectively higher p_T where the cross section is orders of magnitude smaller. (It is this effect that yields large jet/single ratios, since the (quark or gluon) jet trigger is not suppressed by this effect.) On the other hand, if the pion trigger emerges directly from the subprocess (as in the CIM $Mq \to \pi q$ subprocesses) then there is no trigger bias suppression. Thus for some range of p_T, the "higher twist" QCD-CIM subprocesses will be numerically important. Ignoring (logarithmic) scale-violating effects (see Chapter II) the cross sections have the representative forms (see Fig. 1)

$$\text{QCD-Born:} \quad \frac{d\sigma}{d^3p/E}\,(pp \to \pi X) \sim \frac{\alpha_s^2}{(100)p_T^4}\,(1 - x_T)^9 \qquad (2.2)$$

versus

$$\text{QCD-CIM:} \quad \frac{d\sigma}{d^3p/E}\,(pp \to \pi X) \sim \frac{\alpha_M^2}{p_T^8}\,(1 - x_T)^9 \qquad (2.3)$$

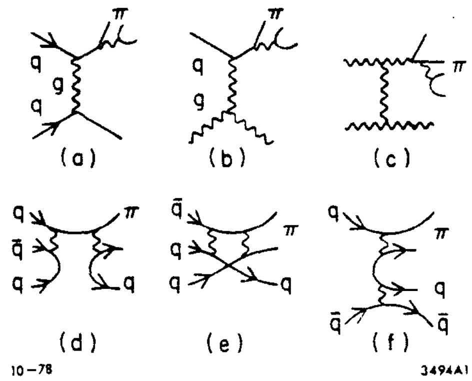

Fig. 1. QCD hard scattering subprocesses for $pp \to \pi X$. In (a),(b) and (c) the π is formed after the hard scattering via quark or gluon fragmentation. In (d) and (e), the "higher twist" CIM contributions, the meson is formed before the hard scattering. Diagram (f) represents the "fusion" CIM $q\bar{q} \to \pi + M$ contribution.

The critical question is determining the magnitude of each contribution.

In principle, it is straightforward to determine the normalization of the $2 \to 2$ QCD subprocess contributing to the inclusive cross section, since α_s and the structure functions are to a large extent determined (although there is some uncertainty in determining the gluon distributions in hadrons). The effect of the k_T distributions of the hadronic constituents is controversial. An essential point ignored in many model calculation is that the interacting constituents are always off the mass shell and spacelike:[17]

$$k^2 = -\frac{\vec{k}_T^2 + \tilde{m}^2}{1-x} \qquad (2.4)$$

where $\tilde{m}^2$ is a linear combination of squares of spectator and incident hadron masses (see Chapter II). The off-shell kinematics ensure that the gluon pole in the $qq \to qq$ amplitude never occurs in the physical region, and serve to damp out the effects of large k_T. In partice, one finds that k_T fluctuations do not increase the inclusive cross section by more than a factor of 2 for $p_T \geq 2$ GeV, even if we assume very large mean $k_T \sim$ 850 MeV Gaussian smearing.[18] A representative calculation is shown in Fig. 2. (If one uses on-shell kinematics, the cross section can be increased by an arbitrary amount depending on a cut-off.) Off-shell kinematics are of course required whether one uses covariant Feynman amplitudes or time-ordered perutrbation theory.

The cross section for subprocesses such as $qM \to qM$ has the form[19]

$$\frac{d\sigma}{dt}(qM \to qM) = \frac{\pi\alpha_M^2}{su^3} \qquad (2.5)$$

corresponding to the QCD amplitude shown in Fig. 1(d). The $qM \to qM$ amplitude falls as s^{-1} at fixed u because of the exchanged fermion in the u-channel. The power fall-off at fixed center-of-mass angle agrees with the dimensional counting rules $d\sigma/dt \propto s^{-(n-2)}$ where n (= 6 here) is the number of active fields in the initial and final state.[20] The constant α_M is proportional to $\alpha_s(p_T^2)$ times the meson wavefunction at the origin. It can be fixed phenomenologically (to

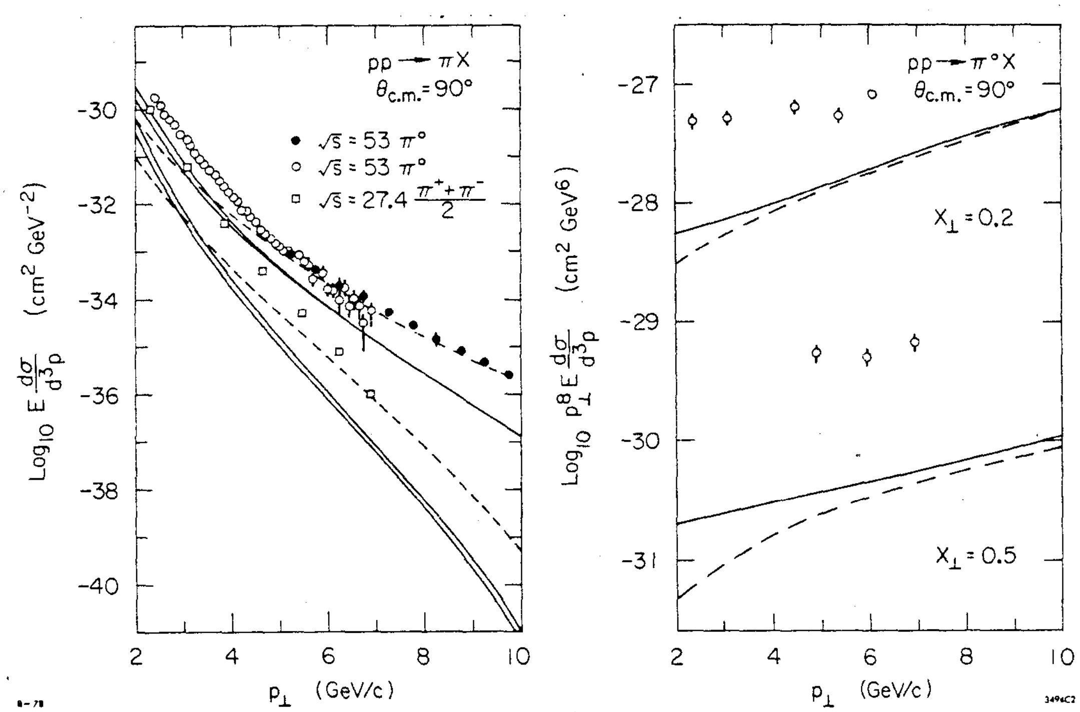

Fig. 2. (a) Data and QCD contributions for $Ed\sigma/d^3p$ ($pp \to \pi X$) at $\theta_{cm} = 90^o$. The dotted line has no scale violations or k_T fluctuations. The lower solid curve indicates scale violations in the structure functions and α_s. The upper solid curve indicates scale violations plus k_T fluctuations calculated with off-shell kinematics. (b) QCD results for $p_T^8\, Ed\sigma/d^3p$ ($pp \to \pi^o X$). The dashed curves indicate scale violations. The solid curves indicate scale violations plus off-shell k_T fluctuations. (From Horgan and Scharbach, Ref. 18.) The sum of QCD plus CIM diagrams give a good fit to the data. See Figs. 5 and 8.

within a factor of ~2), since the $qM \to qM$ amplitude enters directly in the meson elastic form factor and meson-proton elastic scattering at large momentum transfer (see Fig. 3). In a recent paper, Blankenbecler, Gunion and I have found that within errors of order ±50%, $\alpha_M \cong 2\ \mathrm{GeV}^2$.[19]

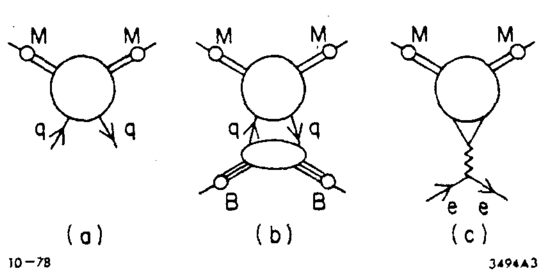

Fig. 3. Contribution of $qM \to qM$ amplitude (a) to meson-baryon scattering (b) and the meson form factor (c).

In order to determine the size of the contribution of the $Mq \to Mq$ subprocess to the $pp \to \pi X$ (see Fig. 4) we also need the normalization of $G_{M/q}(x)$, the distribution of virtual $q\bar{q}$ states in the proton. (The same normalization enters virtual meson-

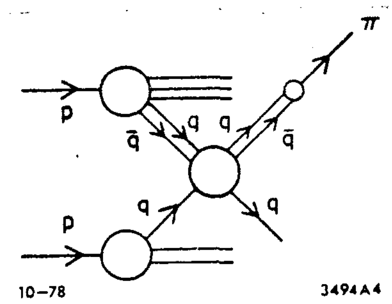

Fig. 4. The CIM $Mq \to \pi q$ contribution to $pp \to \pi X$ at large p_T. The virtual meson M is a $q\bar{q}$ component of the nucleon.

induced reactions, such as Deck or Drell diagrams in low t hadronic physics and the height of the meson plateau in forward reactions.) We have assumed a normalization such that ~1/2 of the $\bar{q}$ sea can be identified as constituents of the virtual $q\bar{q}$ states.

With these normalizations, we find that contributions (B) are in fact consistent with the normalization of FNAL[21] and ISR data[22] for $pp \to \pi X$ up to $p_T \sim 8$ to 10 GeV. At that point we predict the $2 \to 2$ QCD -- Born subprocesses contributions (A) will cross over and dominate the inclusive cross section.[19,22] (See Fig. 5.) Moreover, we note the following:

(1) The best power-law fit to the Chicago-Princeton[21] FNAL data is

$$E \frac{d\sigma}{d^3p} (pp \to \pi^+ X) = \frac{1}{p_T^{8.2 \pm .5}} (1 - x_T)^{9.0 \pm 0.5} \tag{2.6}$$

is agreement with the predicted CIM powers.

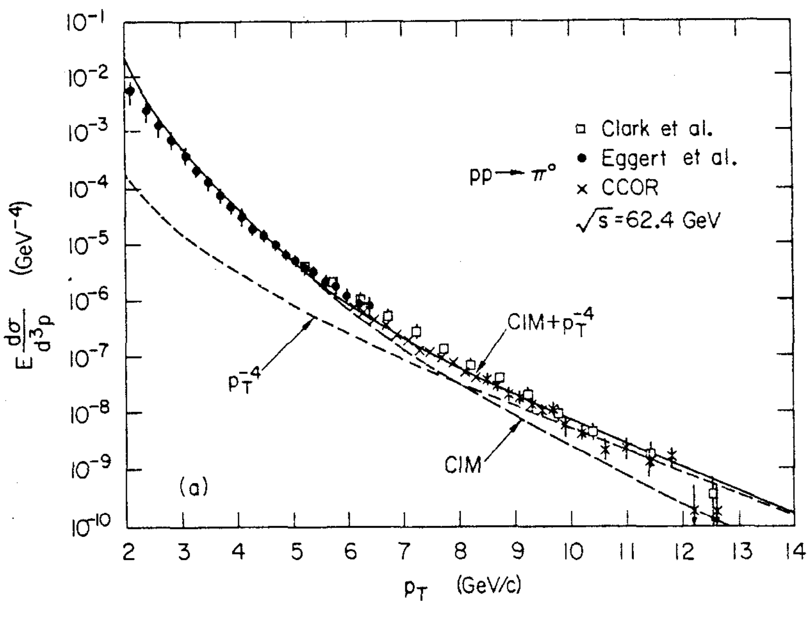

Fig. 5. Comparison with data of CIM plus QCD (p_T^{-4}) contributions to the $pp \to \pi^0 X$ cross section. Scale-breaking is neglected and $\alpha_s = .15$ in the QCD term. (From Jones and Gunion, Ref. 23.)

(2) The best fit[24] to the angular distribution of the subprocess in $pp \to \pi X$ is $d\sigma/dt \propto 1/su^3$ or $1/st^3$ in agreement with the predicted CIM form.

(3) The CIM mechansim predicts that the trigger particle usually emerges alone without same-side correlated particles, or from the decay of resonances, especially the ρ. This is in excellent agreement with the results of the British-French-Scandinavian[25] group's experiment at the ISR, who find that in ~85% of the events with a 4 GeV trigger, the trigger particle is unaccompanied by same-side charged particles (aside from the usual low momentum background). The small growth of the same-side momentum with the trigger p_T observed in the experiment indicates that on average more than 90% of the trigger momentum is carried by the trigger pion -- much larger than the ~75% expected from q or g jet fragmentation.[26] The BSF data clearly does not support the hypothesis that the same-side jet is a quark or gluon jet.

(4) The $qM \to qM$ subprocesses implies that flavor is generally exchanged in the hard scattering reaction.[27] For example, consider the quark interchange and $q\bar{q} \to M\bar{M}$ fusion contributions to $pp \to K^{\pm}X$ shown in Fig. 6. The average charge of the recoil quark is slightly positive for the K^+ trigger and $> +1/3$ for the case of the K^- trigger. Thus the charge and flavor of the away-side jet in the CIM can be correlated with the flavor quantum numbers of the trigger. In contrast, gluon exchange diagrams predict very small[26] flavor correlations between the away-side and same-side systems. The data from the BSF-ISR group (see Fig. 7) for various charge triggers at 90° show striking flavor correlations, especially for K^- and $\bar{p}$ triggers, in general, agreement with the above expectations for the quark exchange processes of the CIM model. (A possible difficulty, however, may be the absence of a strong difference in the away-side +/- ratio for π^+ and π^- triggers. This may be due to the fact that resonance decays, particularily $\rho^0 \to \pi^+\pi^-$, dilute the charge correlations.) It should be emphasized that the CIM terms are not maximal for back to back configurations because of the difference in q and M distributions. [This could explain why charge correlations are

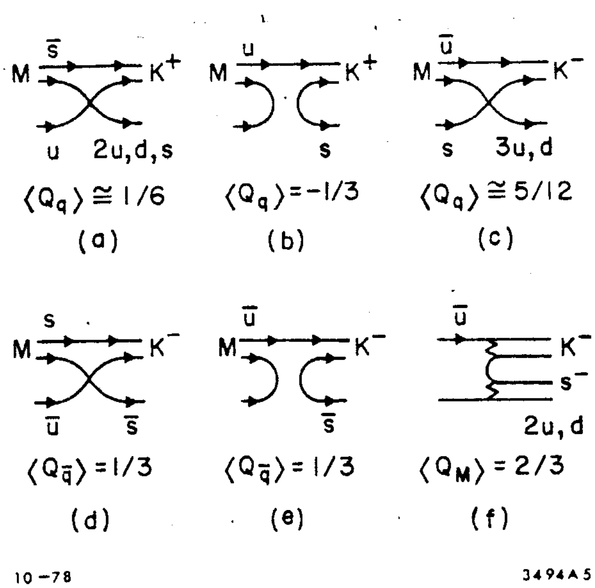

Fig. 6. Analyses of charge flow in CIM diagrams for $pp \to K^{\pm}X$. Quark exchange in the subprocess implies charge correlations between the trigger and away-side jet.

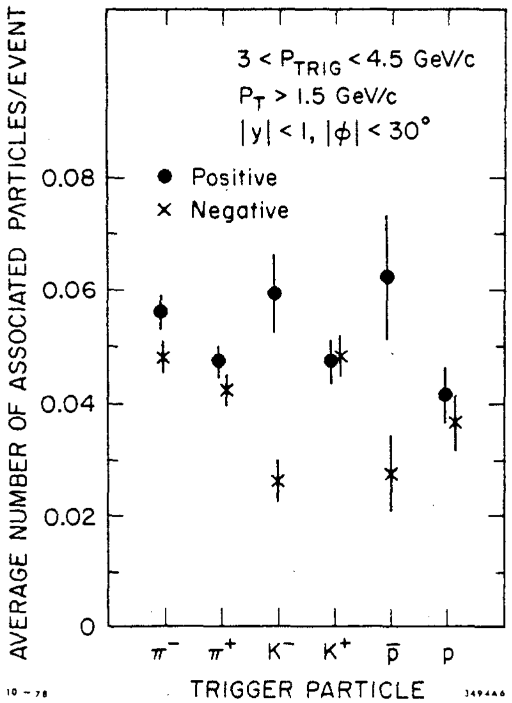

Fig. 7. Number of fast positive and negative particles on the side-away from a 90° trigger for various trigger type. (From Ref. 25.) The gluon exchange QCD diagrams give an away-side jet nearly independent of the trigger type. See R. Field, Ref. 10.

strongest away from zero rapidity on the away-side in the BSF-ISR[25] experiment and why only minimal flavor correlations are observed in the FNAL experiment of R. J. Fisk et al.,[28] who only look at particles directly opposite a 90° trigger. The correlations will also be reduced because of the nuclear target.]

In each case we would expect that these charge correlations will disappear at very high p_T when the $2 \to 2$ QCD -- Born subprocesses become dominant. It is interesting to note that for K^- and $\bar{p}$ triggers, the cross-over point is predicted by Jones and Gunion[23] to occur (for pp collisions) at a relatively small p_T (~ 4 to 5 GeV at ISR energies) due to the rapid fall-off of the CIM terms as $x_T \to 1$ for these triggers. Thus there is a rich, dynamical structure controlled by the p_T and x_T kinematics which can be unraveled by quantum number correlations.

(5) In the case of $pp \to pX$, the dominant CIM subprocess is the $qB \to qp$ subprocess. The theoretical prediction is $Ed\sigma/d^3p\ (pp \to pX) \propto p_T^{-12}(1-x_T)^7$. The Chicago-Princeton[21] fit at 90° in fact gives $p_T^{-11.7}(1-x_T)^{6.8}$ at FNAL energies, $p_T < 7$ GeV with uncertainties in the exponent of order ±0.5. We emphasize that a successful model for single particle production must account for <u>both</u> high p_T meson and baryon data. There does not seem any way to account for the $pp \to pX$ scaling behavior in terms of $2 \to 2$ QCD subprocesses without enormous scale-breaking in the $q \to p$ distribution function; we note that data from DESY for $e^+e^- \to \bar{p}X$ appears to be reasonably consistent with scale-invariance. On the other hand, we find that the normalization of the $Bq \to Bq$ subprocess required here is consistent with elastic $pp \to pp$ scattering and the proton form factor.[19] In addition, at $\theta_{cm} = 90^{\circ}$, $x_T > 0.6$, we predict that the direct scattering process $pq \to pq$ (where the incident proton itself scatters in the subprocess) should become dominant, leading to $p_T^{-12}(1-x_T)^3$ behavior. The direct scattering contribution to inclusive $pp \to pX$ connects smoothly to elastic scattering $pp \to pp$, in agreement with the Bjorken-Kogut "correspondence principle" arguments.[29]

Combining the QCD 2-2 Born subprocess contributions with the CIM (higher twist QCD) contributions leads to a combined prediction for $pp \to \pi^+ X^-$ of the form $(\theta_{cm} = 90^o)$[19]

$$E \frac{d\sigma}{d^3p}(pp \to \pi^+ X^-) = \alpha_s(p_T^2)(0.035)\frac{(1-x_T)^9}{p_T^4} + (9)\frac{(1-x_T)^9}{p_T^8}, \tag{2.7}$$

in GeV units. The 0.035 factor includes the suppression factor due to trigger bias[16] from $q \to M+q$ fragmentation as discussed above. (The factor of 9 in the CIM term is computed using $\alpha_M = 2\ \mathrm{GeV}^2$ and an estimated factor of 2 from resonance decay contributions to inclusive π^+ production.) The $(1-x_T)^9$ power comes from convolutions of valence distributions $G_{q/p}(x)$ with $(1-x)^3$ fall-off and $G_{\pi/q} \sim (1-x)^5$. Asymptotic freedom,[5] spin correlations, etc. can increase the effective power to $(1-x_T)^{10 \text{ or } 11}$. Thus at $p_T \sim 10$ GeV, the $2 \to 2$ subprocesses are predicted to be dominant, the power of p_T for $\pi^{\pm,o}$, K^+, and production should decrease to p_T^{-6} and then asymptotically approach p_T^{-4} scaling, modulo QCD logarithmic radiative corrections. At these values of p_T all the canonical QCD predictions characteristic of the Born diagrams should hold; in particular the same-side system will cease to be dominated by single particles, and flavor correlations between the trigger and away-side system will tend to zero. An important prediction of QCD is the eventual dominance of gluon jet recoil.[11,26]

We note that recent ISR data[22] for the $pp \to \pi^o X$ cross section for $6 < p_T < 12$ GeV are indeed consistent with a sum of terms of the form of Eq. (2.7) (see Fig. 8). For $p_T < 8$ GeV, the experimental data are consistent with dominance of the CIM terms. We emphasize that the predicted QCD $2 \to 2$ Born contributions alone are at least a factor of 5 below the data for $p_T \sim 4$ GeV, even allowing for a factor of 2 from k_T smearing corrections and uncertainties in the effective value of α_s; in any event these contributions are inconsistent with all of the features of the data, (1) through (5) discussed above.

An important theoretical question is how to systematically include the effects of higher particle number hard-scattering subprocesses $2 \to n$ and even $m \to n$. In a recent paper by Casewell, Horgan, and myself[18] we showed that for ϕ^3 field theory, the inclusive cross section for $A+B \to C+X$ can be computed systematically in terms of a sum of incoherent hard scattering contributions, as expected by parton-model considerations. In the ϕ^3 model all effects associated with large k_T in the incident wavefunction are automatically include when the higher order subprocesses are taken into account. Subprocesses with higher number of active fields suffering the large momentum transfer give higher powers of p_T fall-off.

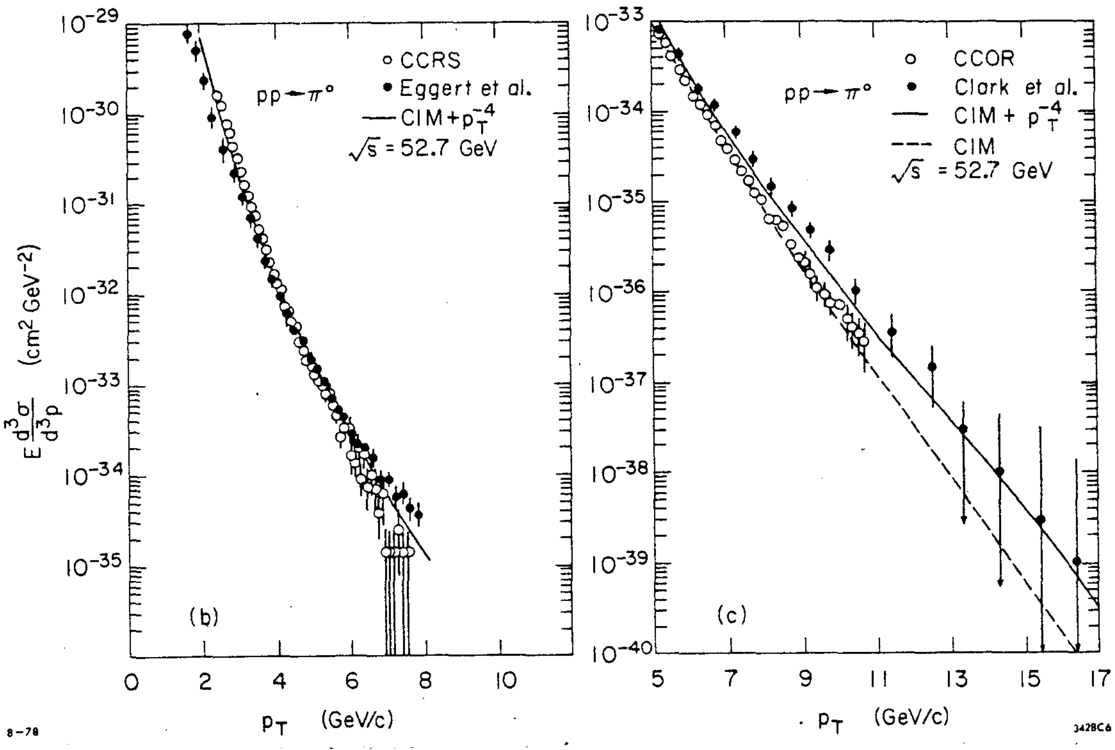

Fig. 8. Comparison with data of CIM plus QCD (p_T^{-4}) contributions to the $pp \to \pi^0 X$ cross section. Scale-breaking is neglected and α_s = .15 in the QCD term. (From Jones and Gunion, Ref. 23.) The data may include contributions from direct photons, $pp \to \gamma X$.

The situation in QCD is best illustrated by an example (see Fig. 9). A Feynman diagram which corresponds to $qq \to qq$ scattering with gluon bremsstrahlung yields contributions to both the $qq \to qq$ hard scattering subprocess (when the emitted gluon g_1 is parallel to q_1) and to the $qg \to qg$ subprocess (when the exchange gluon g_2 is at low k_T relative to q_2). The contribution where the q_3, q_4, and g all emerge at different θ_{cm} is suppressed by a power of log p_T^2. Note that (1) off-shell kinematics are required in order to obtain the correct contribution to the $gq \to gq$ subprocess; (2) it would be double-counting to include both k_T fluctuations to $qq \to qq$ scattering plus the $gq \to gq$ subprocess; and (3) the leading logarithmic corrections to the $qq \to qq$ scattering are already included when the measured $G_{q/p}$ structure function is used. A consistent treatment in QCD requires simultaneous considera-

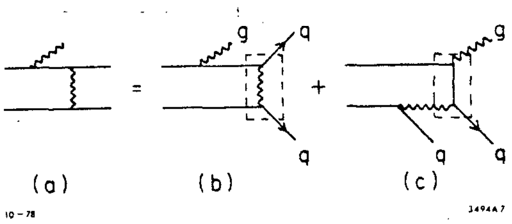

Fig. 9. Illustration of hard scattering expansion. The Feynman amplitude (a) contains contributions from (a) $qq \to qq$, and (b) $gq \to gq$ subprocesses.

tion of the hadronic wavefunctions, off-shell effects, and the k_T fluctuations implicit in higher particle number subprocesses.

The theoretical origin of the k_T distribution of the quark and gluon distributions in hadrons is complicated, since there are clearly several mechanisms at work:

(a) The tail of the hadronic wavefunction at large k_T due to constituent recoil gives a contribution of order

$$\frac{dN}{dk_T^2} \sim \frac{\alpha_M}{k_T^4} \qquad (m^2 << k_T^2 << p_T^2) \tag{2.8}$$

(b) Radiative corrections due to single gluon recoil gives

$$\frac{dN}{dk_T^2} \sim \frac{\alpha_s(k_T^2)}{k_T^2} \qquad (m^2 << k_T << p_T^2) \tag{2.9}$$

and eventually will dominant over (a). This contribution can also be identified with $2 \to 3$ QCD subprocesses.

(c) In any inclusive process in which color is virtually separated the radiated soft gluons taken together give an effective k_T distribution. According to the analysis of Dokshitser, D'yakanov, and Troyan[30] for the Drell-Yan process, the effective distribution has a computable Gaussian-like shape.

(d) The intrinsic k_T distribution of the hadronic wavefunction due to binding and ohter non-perturbative effects. The recent bubble chamber measurements of the final state hadron distribution in deep inelastic neutrino-proton scattering reported at this meeting by Vander Velde[31] shows that the intrinsic k_T of the constituents are in fact small; the fast hadrons near $x_F \cong -1$ in the $W^{\pm}$- proton cm frame (from the spectator "qq" jet) have $\langle k_T^2 \rangle \cong 0.1$ GeV^2. The large values of k_T observed in Drell-Yan and large p_T reactions (from p_{out} distributions) thus must be attributed to a combination of the mechanics (a), (b) and (c).

As we discussed, the CIM (higher twist QCD) diagrams can temporarily dominate the $2 \to 2$ Born subprocess contributions because of the trigger bias in single particle high p_T reactions. In the case of jet triggers, the trigger bias is absent, and the QCD Born terms are expected to be dominant even at $p_T \sim 4$ GeV. Thus jet experiments can provide a direct tool to check the basic form of QCD dynamics, verify the form and magnitude of the tri- and quartic-gluon interactions, etc. At present, there is a great deal of uncertainty how to define a jet trigger, particularly because of possibly striking differences in the structure of gluon and quark jets. The study of jet production in two photon physics and the recoil system in deep inelastic scattering should be helpful for establishing workable definitions for jet triggers.

The CIM-QCD approach to large p_T dynamics, combined with dimensional counting rules for determining the leading power behavior, makes a large number of phenomenological predictions (see Refs. 19, 23). Thus far, I am not aware of any serious conflicts with data. In particular, the observed particle ratios such as $pp \to K^- X/pp \to K^+ X$ and beam ratios $\pi p \to \pi X/pp \to \pi X$ are not inconsistent with the CIM (although in the latter case, the situation is complicated by the presence of several competing subprocesses). It is very interesting that corrections to scaling can now be systematically evaluated in perturbative QCD for the higher twist/CIM subprocesses (see Chapter II).

3. Photon Production at Large P_t

In addition to $\gamma\gamma$ collisions (see Chapter III), other photon-induced reactions such as $\gamma p \to \pi X$, $\gamma p \to \gamma X$, and $\gamma p \to$ jet X are sensitive to "direct" QCD reactions such as $\gamma q \to Mq$, and $\gamma q \to \gamma q$, where the incident photon participates in the hard scattering subprocess (and no forward hadrons are produced)[32] as well as standard QCD or CIM subprocesses such as $qq \to qq$, $qM \to qM$, and $qM \to \gamma M$, where the perturbation QCD "anti-scaling" structure function of the incident photon is important.

Photon production at large p_T can also be used as an important probe of the underlying hard scattering subprocesses.[1,2] Discarding photons which are produced from hadron decay ($\pi^0 \to \gamma\gamma$, $\eta^0 \to \gamma\gamma$, etc.), we can distinguish several mechanisms in QCD:

(a) QCD Born contributions with quark fragmentation, e.g.: $e^+e^- \to q\bar{q}$, $qq \to qq$, $gq \to gq$ with $q \to \gamma q$. The $G_{\gamma/q}(x,Q^2)$ fragmentation distribution has the Witten[33] anti-scaling form and is nearly flat in x until x very close to 1. If a QCD 2-2 subprocess dominates both π and γ production, then

$$\frac{\frac{d\sigma}{d^3p/E}\,(pp \to \gamma X)}{\frac{d\sigma}{d^3p/E}\,(pp \to \pi X)} \sim \frac{G_{\gamma/q}(x_T)}{G_{\pi/q}(x_T)} \sim \frac{\alpha}{1 - x_T} \tag{3.1}$$

at $\theta_{cm} = 90^o$, independent of p_T.

(b) <u>Direct</u> QCD Born contributions, from subprocesses such as:

$$gq \to \gamma q \qquad \text{and} \qquad q\bar{q} \to \gamma g \quad .$$

In these processes the photon is produced in the subprocess itself. Since there are no accompanying trigger jet hadrons one can easily distinguish such reactions from fragmentation processes.[2] These reactions can also be important for producing massive lepton pairs at large transverse momentum.

(c) CIM-type subprocesses, such as $Mq \to \gamma q$, where the incident meson M is a correlated $q\bar{q}$ pair in the incident hadron wavefunction.

Both processes (b) and (c) can dominate over (a) for moderate p_T because of the absence of trigger bias suppression. The nominal scaling laws are[2]

$$E \frac{d\sigma}{d^3p}(pp \to \gamma X) \sim \begin{cases} \alpha_s^2 \, \alpha_\gamma \, \dfrac{\varepsilon^8}{p_T^4} & \text{(a) } qq \to qq, \text{ etc.} \\ \alpha_s \, \alpha \, \dfrac{\varepsilon^8}{p_T^4} & \text{(b) } gq \to \gamma q \\ \alpha_M \, \alpha \, \dfrac{\varepsilon^9}{p_T^6} & \text{(c) } Mq \to \gamma q \end{cases} \qquad (3.2)$$

where $\alpha_\gamma \sim \alpha/\alpha_s(p_T^2) \sim \alpha \log p_T^2/\Lambda^2$ and $\varepsilon = 1-x_T$. A systematic discussion of these contributions and their relative magnitude is discussed in Ref. 2. We found that with conventional parameterizations, the CIM contributions (c) exceed the QCD (a)+(b) terms until $p_T^\gamma \sim 8$ GeV at $\sqrt{s} = 33$ GeV, and until $p_T^\gamma \sim 9$ GeV at $\sqrt{s} = 61$ GeV. The ratio of γ to pion production (parameterized as ε^9/p_T^8) is shown in Fig. 10. For $p_T \lesssim 8$ GeV where the CIM subprocesses dominate both pion and photon production, we predict at 90° the cross section ratio:[19,2]

$$\frac{\gamma}{\pi} \cong 0.007 \; p_T^2/\text{GeV}^2$$

roughly independent of s. This dependence of p_T and s should be readily distinguishable from the $\gamma/\pi \sim \alpha_\gamma/(1-x_T)$ dependence characteristic of conventional QCD calculations. We also note that the predictions of Fontannaz[34] and Blankenbecler et al.[35] which are based on the $Mq \to \gamma^* q$ subprocess appear to account for a large share of the p_T distribution of messive lepton pairs.[36]

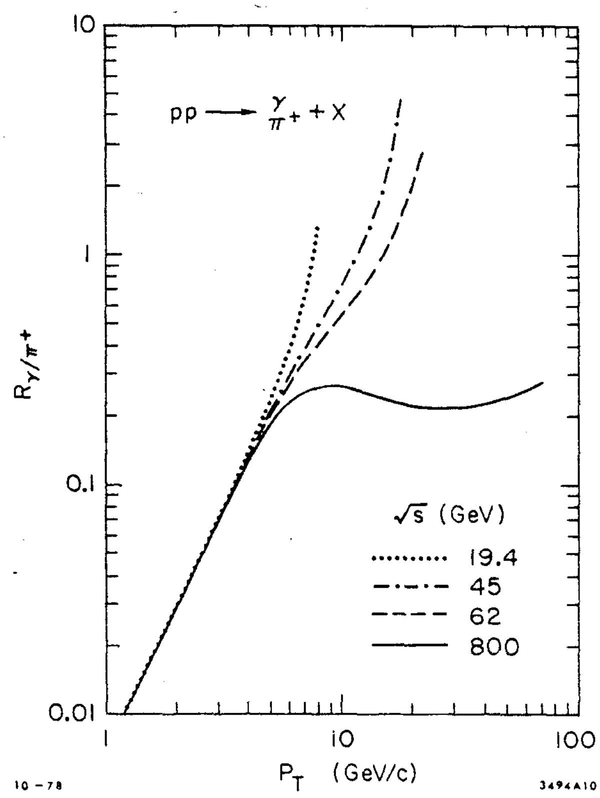

Fig. 10. Predicted ratio from QCD plus CIM contributions for γ/π in pp collisions. (From R. Rückl et al., Ref. 2.)

4. Photon and Gluon Jet Production

It should be emphasized that direct large p_T photon production at the magnitude discussed here is an essential prediction of the hard-scattering approach to hadron dynamics. In particular, since photons and gluons enter subprocesses in a similar manner, there is a close relationship between gluon jet and direct photon production. For example, consider the subprocesses[11]

$$\frac{d\sigma}{dt}(gq \to gq) = \frac{\pi\alpha_s^2}{s^2}\left[-\frac{4}{9}\left(\frac{s}{u}+\frac{u}{s}\right)+\frac{s^2+u^2}{t^2}\right] \qquad (4.1)$$

and

$$\frac{d\sigma}{dt}(gq \to \gamma q) = \frac{\pi\alpha\alpha_s e_q^2}{3s^2}\left[-\left(\frac{s}{u}+\frac{u}{s}\right)\right] \qquad (4.2)$$

At 90°, this implies

$$\frac{\frac{d\sigma}{d^3p/E}(pp \to \gamma X)}{\frac{d\sigma}{d^3p/E}(pp \to gX)} = \left(\frac{1}{22}\right)\frac{\alpha}{\alpha_s(p_T^2)} \qquad (4.3)$$

from these subprocesses alone. Direct photons and gluon jets from these contributions have the same scaling laws, independent of structure functions, k_T smearing, etc. We note that the $gq \to gq$ subprocess gives ~1/4 of the total jet production cross section from all QCD $2 \to 2$ subprocesses.[26] Therefore we have a lower bound

$$\frac{\frac{d\sigma}{d^3p/E}(pp \to \gamma X)}{\frac{d\sigma}{d^3p/E}(pp \to \pi X)} \geq \left(\frac{\text{Jet}}{\pi}\right)_{\text{expt}} \cdot \frac{\alpha}{88\alpha_s(p_T^2)} \qquad (4.4)$$

For example, if the jet/π ratio is of order 300 (to 600) as in the FNAL E260 experiment[37] ($p_T \sim 4.5$ GeV, $E_{Lab} = 200$ GeV), then the γ/π <u>lower</u> bound is 12.5% (to 25%). Conversely, the experimental upper bound for γ/π of $(.55 \pm .92)\%$ as reported by J. H. Cobb *et al.*[38] at $2 < p_T < 3$ GeV, $\sqrt{s} = 55$ GeV implies an upper bound for jet/π production of order 30, which is in severe disagreement with QCD expectations and the trend of experimental results. Thus the production of direct photons may provide one of the most important constraints on QCD subprocesses.

5. Color and Hadron Multiplicity

One of the most intriguing problems in QCD is how to unravel the mechanisms which control the development of hadron multiplicity in large momentum transfer reactions. The "inside-outside" space-time development of hadron production as discussed by Casher, Kogut, and Susskind[39] and Bjorken[40] for $e^+e^- \to q\bar{q} \to$ hadron is consistent with causality and confinement. This picture implies that the fastest hadrons (which contain the valence quarks) are formed last, and the slow polarization cloud first. Weiss and I,[41] building on earlier work,[42] have shown that in such a picture, the charge of a quark jet (on the average) is equal to the charge of parent quark plus the average charge of anti-quarks in the sea:

$$Q_{jet} = Q_q + \langle Q_{\bar{q}} \rangle_{sea} \tag{5.1}$$

Here Q_{jet} is obtained by integrating the charge density in the jet starting from y_0 (anywhere in the central region) to Y_{max}. Gluon jets have $Q_{jet} = 0$. These results hold for all conserved quantum numbers Q.

The inside-outside description of jet dynamics leads to the following ansatz for QCD:[3] Soft hadron production in a hard scattering reaction depends only on the effective color separation. Accordingly, two reactions which initially separate any two 3 and $\bar{3}$ systems (q, $\bar{q}$, $\overline{qq}$, qq, etc.) will have the same distribution of hadrons in the central region. (Only the fragmentation region discriminates the flavor and composition of the jet.) Thus we expect the same multiplicity distributions (e.g., plateau height) in the central region for the hadron system X in $e^+e^- \to X$, $\gamma^* p \to X$, and $pp \to \mu^+\mu^- + X$ (Drell-Yan mechanism), given the same rapidity separation of the 3 and $\bar{3}$ systems. For large p_T reactions, the subprocess $qq \to qq$ leads to four 3 or $\bar{3}$ jets. The multiplicity and associated coherence effects associated with these jets can be computed in analogy with the soft-photon production formulae of QED for the corresponding charge separation reaction, positronium + positronium $\to e^+ + X$ [$e^+e^\pm \to e^+e^\pm$ subprocesses]. The net multiplicity corresponds to 4 quark jets, with coherent enhancement in the interference zone.

An important consequence of the color separation ansatz is that gluon (color 8) jets must have a different soft hadron spectrum than quark jets. In fact, for $N_c \to \infty$, the color separation for a gluon jet is the same as two incoherent quark jets. More generally, the number of soft gluons bremsstrahlunged from a gluon source compared to a quark source is given by the ratio of Casmir operators for the adjoint and fundamental representation:[3,4]

$$\frac{\langle n^{soft}\rangle_g}{\langle n^{soft}\rangle_q} = \frac{2}{1 - N_c^{-2}} = \frac{9}{4} \quad \text{for color SU(3)} \tag{5.2}$$

Thus we expect that the plateau height for soft gluons (or sea quarks) in the gluon jet is 9/4 that of quark jets (i.e., a color octet has 3/2 the "color charge" of the color triplet). If we assume the density of produced hadrons is linearly related to the sea-quark density, then gluon jets will have more than twice as many soft hadrons in the central region compared to quark jets. Further,[43,44] the energy of a gluon jet will be contained in a larger solid angle due to its increased "straggling" -- again due to the 9/4 color factor. The leading particle distribution in a gluon jet will also be depleted more strongly by soft gluon radiation.

On the other hand the dependence of hadron multiplicity on soft gluon or quark production may not be as strong as linear. For example, the lower density of $g \to q\bar{q}$ pairs in a color triplet jet implies that the average cluster (singlet $q\bar{q}$) mass will be of higher mass than clusters due to the more copious bremsstrahlung from the color octet jet. Since the heavier clusters decay with a higher multiplicity, the net difference between quark and gluon multiplicities may not be as severe as indicated by QCD perturbation theory.[45] Nevertheless, taking into account their different structure at the short distance level, it would be very surprising if the hadron distribution from quark and gluon jets turned out to be identical.

QCD and "Hole" Partons

Several years ago Bjorken[46] postulated the concept of a "hole" parton to describe the development of the final state multiparticle distribution after a deep inelastic lepton reaction. It is an interesting question whether this parton model ansatz has an analogue in QCD.

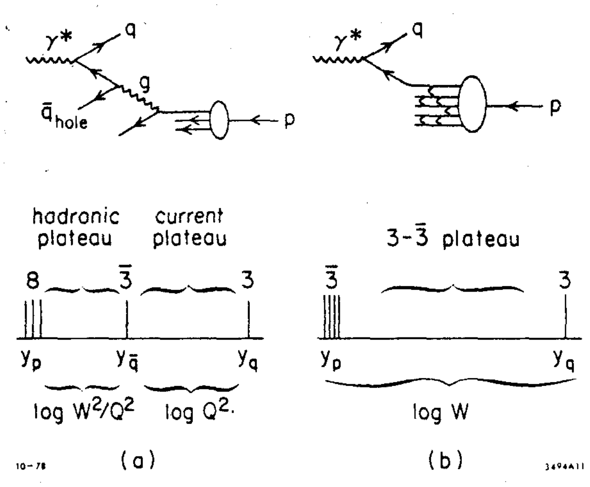

Fig. 11. Illustration of final state hadron distribution deep inelastic lepton scattering on a sea quark arising from (a) gluon bremsstrahlung or (b) a $(q\bar{q}\ qqq)$ Fock state.

A common phenomenological assumption is that sea quarks in a hadron arise as low-mass pair states created from gluon bremsstrahlung. If this perturbative picture is correct, then after a sea quark with rapidity y_0 is struck by a deep inelastic γ or W, the spectator system consists of (1) an antiquark (hole parton) at $y \sim y_0$ with quantum numbers opposite to those of the struck quark, and (2) a leading particle system with the rapidity of the target hadron, but with color 8 (see Fig. 11(a)). There are thus two rapidity regions created from the color neutralization:

(a) a "current" plateau region of length log Q^2 between the 3 and $\bar{3}$, and (b) an "hadronic" plateau of length log (W^2/Q^2) between the 8 and hole parton $\bar{3}$. The density of soft gluons created in the neutralization of the 8-8 system will be 9/4 that of the 3-$\bar{3}$ separated system; thus we expect the height of the hadronic plateau to be higher than that of the current plateau; i.e., the hadronic multiplicity will be a function of both W^2 and Q^2. Despite these expectations, data from deep inelastic electron and neutrino reactions indicate that the current and hadron multiplicity plateaus have equal heights. We note that dual string picture also predicts that the "hadronic" plateau should be twice as high as the "current" plateau.

There is however an alternative description of the proton gluon and quark distribution, which requires giving up a simple perturbative picture of the $q\bar{q}$ sea.[47] The hadronic state is evidentally a complicated coherent color state: all constituents tend to have the same rapidity in order that the system remains a coherent singlet over the semi-infinite time before collision. The virtual gluon, quark, and antiquark states are thus continually exchanging momentum. When a virtual sea quark is struck at y_0, the remaining state is that of a coherent $\bar{3}$ at the original rapidity Y of the target. Because of the exchange of momentum in the initial state, there is no special reason for a $\bar{q}$ with opposite quantum numbers to be at the struck quark rapidity, and there is no "hole" parton (see Fig. 11(b)). Furthermore, there is no separate current or hadronic plateaus; the multiplicity should only depend on log W^2, in agreement with data.

The question of the color and quantum number content of the hadronic state before and after a deep inelastic reaction is a fascinating subject, which deserves much more theoretical and experimental attention. The associated multiplicity in massive lepton pair production events could be an ideal laboratory for studying this problem since both valence and sea distributions of mesons and baryons can be probed, and a comparison can readily be made with either normal events or low-mass pair events.

Another important problem related to the detailed nature of the hadronic wavefunction concerns the question shadowing in deep inelastic events on nuclei. It is still not settled theoretically or experimentally whether the nucleon number A^{α} dependence is controlled by Bjorken x or q^2. Analyses in terms of the parton model are given in Refs. 40 and 48.

6. The Forward Fragmentation Region and Short-Distance Dynamics

Although hadronic scattering in the forward direction is normally not regarded as a probe of quark dynamics, the forward and backward fragementation regions in $A+B \to C+X$ at $x_L^C \sim \pm 1$ deserves special attention. In order for C to have nearly all the momentum of A or B, there must be the exchange of large momentum transfer between constituents which are far off-shell. The forward systems produced in low p_T reactions can be regarded, in a general sense, as hadronic jets and many of their properties (multiplicity, k_T

distributions, quantum number correlations) are not dissimilar from jets in e^+e^- annihilation or large p_T reactions.[3] Blankenbecler and I[49] have emphasized the unity and continuity of physics throughout the Peyrou plot; in particular, the dynamics at the quark and gluon level for large p_T reactions at $x_R = p_C/p_C^{max} \sim 1$ at fixed θ_{cm} must connect smoothly with forward reactions at $x_L \sim 1$ as $\theta_{cm} \to 0$ or π. In particular, Ochs[50] has noted the phenomenological similarity between particle ratios at $\theta_{cm} = 90^o$ and 0^o in pp collisions.

The first suggestion that the behavior of the forward fragmentation region in inclusive reactions can be related to the quark distributions in hadrons is due to H. Goldberg.[51] However, the simplest implementation of this idea fails: For example, for the reaction $pp \to \pi^+X$, one can imagine that either before or after an initial soft scattering, a u-quark in the proton, with the distribution $G_{q/p}(x)$ (obtained from deep inelastic lepton scattering) fragments to the fast pion with the distribution $G_{\pi^+/u}$ (obtained from e^+e^- annihilation) (see Fig. 12(a)). Although this ansatz can account for the observed particle ratios in the forward direction, it predicts a too-small and too-steeply falling distribution,

$$\frac{1}{\sigma}\frac{d\sigma}{dx_L}(pp \to \pi^+X) \propto (1-x_L)^5 \qquad \text{(prediction)}^{49} \qquad (6.1)$$

vs.

$$\frac{1}{\sigma}\frac{d\sigma}{dx_L}(pp \to \pi^+X) \propto (1-x_L)^{3.1 \pm 0.5} \qquad \text{(experiment)}^{52} \qquad (6.2)$$

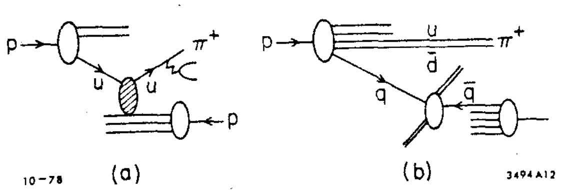

Fig. 12. Production of high energy, low p_T pions in $pp \to \pi^+X$ arising from (a) diffractive or gluon exchange processes or (b) $q\bar{q}$ annihilation of sea quarks.

The prediction (6.1) can also be derived in QCD if one assumes that soft hadronic interactions are represented by gluon exchange.

There is however another possibility:[53] consider the five quark $uud\bar{q}_{sea}q_{sea}$ > component of the proton wavefunction. The sea quark has a flat distribution in rapidity and can be exchanged or annihilated in the target, giving a constant total cross section [see Fig. 12(b)]. (This is the QCD analogue of Feynman's "wee parton" mechanism for high energy interactions.) The distribution of meson systems $u\bar{q}_{sea}$ in the remaining 4-quark state is

$$\frac{1}{\sigma}\frac{d\sigma}{dx_L}(pp \to \pi^+X) \propto G_{\pi^+/uud\bar{d}}(x) \sim (1-x_L)^3 \qquad (6.3)$$

where we have used the QCD-based spectator counting rule,[49,54]

$$G_{a/A}(x) \propto (1-x_L)^{2n_s-1} \qquad (x \to 1) \qquad (6.4)$$

where n_s is the number of bound spectators which are required to stop as $x = (k_0^a + k_3^a)/(p_0^A + p_3^A) \to 1$. Notice that for the gluon exchange mechanism, there are 3 spectators for $pp \to \pi^+ X$, versus 2 spectators for the wee-quark exchange case.

A large number of forward reactions have been measured; the results are generally in good agreement with the powers predicted by the q-exchange mechanisms.[53] It is likely that both soft q and g exchange mechanisms are important in forward reactions; it is just that sea quark exchange is more effective in producing fast particles. Other consequences of this picture, including induced correlations between particles at $x_L = \pm 1$ are discussed in Ref. 53. We also note that two particle correlations at $x_L(1) + x_L(2) \to 1$ are also readily predicted:

$$\frac{dN}{dx_1\,dx_2}\,(pp \to \pi^+\pi^+X) \sim \frac{dN}{dx_1\,dx_2}\,(pp \to \pi^+\pi^-X)$$

$$\gg \frac{dN}{dx_1\,dx_2}\,(pp \to \pi^-\pi^-X) \qquad (6.5)$$

where we utilize the two valence quarks in the proton. Tests of these ideas can illuminate the multi-quark correlations in hadronic wavefunctions. A recent test of the quark spectator rule for the distribution of fast forward particles in large p_T reactions in correlation with various triggers has been given by the CCHK group.[55] There are also a number of successful applications of this rule to nuclear-induced reactions. An alternative parton model for forward-fragmentation processes has been given by Das and Hwa.[56] A comparison between these approaches and applications to Drell-Yan processes is given in Ref. 57.

7. Gluon Jets

The essential property of QCD which distinguishes it from a generalized quark-parton model, is the prediction of jets derived from the initial creation of a gluon quantum. Gluon jets are predicted in e^+e^- annihilation (3-jet decay from $e^+e^- \to q\bar{q}g$) and in deep inelastic scattering ($eq \to eqg$). The identification of multijet events corresponding to such subprocesses is not completely straightforward because of severe backgrounds from subprocesses such as $e^+e^- \to \pi q\bar{q}$; the relatively large $q \to Mq$ coupling dominates the $q \to gq$ process until quite large p_T. Selection of events with high multiplicity could be used to favor gluon jet production.

By comparing the processes $q\bar{q} \to \gamma + g$ and $q\bar{q} \to \mu^+\mu^-$ for high p_T γ or μ^+ production, we can obtain a prediction for gluon jet production which is independent of the initial state:[58]

$$\frac{\dfrac{d\sigma}{d^3p/E}(AB \to \gamma X)}{\dfrac{d\sigma}{d^3p/E}(AB \to \mu^+ X)} = \frac{\frac{4}{3}\alpha_s(p_T^2)}{\alpha}\,\frac{4}{\langle \sin^2\hat{\theta}\rangle} \qquad (7.1)$$

Here $\sin^2\hat{\theta}$ is the subprocess center-of-mass production angle. Low mass $\gamma^* \to \ell\ell^-$ pairs can be used here to avoid backgrounds.

The decay of heavy quark systems $Q\bar{Q}$ such as the Υ into 3 gluons[5] or γ+2 gluons[6] could provide the cleanest test of QCD gluon jet phenomenology. The standard perturbation formulae for positronium decay, updated for color factors gives the branching ratio[59,60]

$$\frac{\Gamma(\Upsilon \to \gamma gg)}{\Gamma(\Upsilon \to ggg)} \cong \frac{36}{5}\left(\frac{e_Q}{e}\right)^2 \frac{\alpha}{\alpha_s(M_\Upsilon^2)} \qquad (7.2)$$

where $Q^2 \cong M_\Upsilon^2$ is the effective off-shell value to be used in the running coupling constant. If $e_Q = 1/3$, the branching ratio is ~3%. Predictions for the angular distributions of the Υ decay plane relative to the beam axis and decay distributions are given in Ref. 6. The $\Upsilon \to \gamma gg$ two-jet channel is particularly interesting since the $gg \to X$ mass can be varied and a direct comparison with SPEAR $q\bar{q}$ jets at the same energy can be made. The predicted spectrum based on perturbation theory as a function of $M_{gg}^2 = M_\Upsilon^2(1-x_\gamma)$, $x_\gamma = p_\gamma/p_{max}$, is shown in Fig. 13. Resonances with the gg quantum numbers (η, η', η_c, glueballs) can be expected to modulate the perturbative prediction over a local region if we assume local duality.

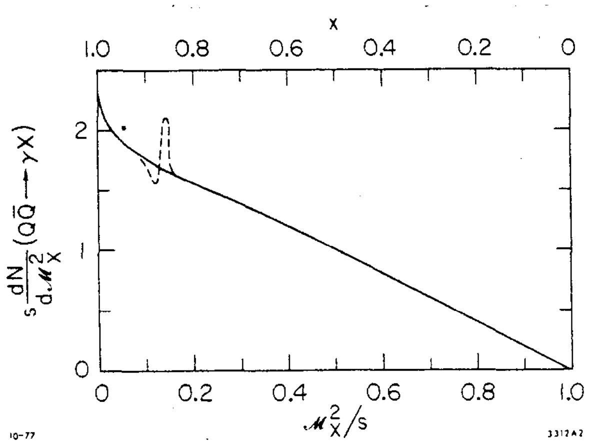

Fig. 13. Decay distributions for $\Upsilon \to \gamma + X$ in $x = 2\omega/M_\Upsilon$ and $\mathcal{M}_X^2/s$ from the simpliest QCD diagrams $\Upsilon \to g+g+\gamma$, and massless gluons. The modulation of a singlet resonance at fixed $\mathcal{M}_X^2$ is shown schematically.

It should be noted that all of these predictions for gluon jet production treat the gluon as strictly massless. Although this is evidently correct for QCD matrix elements, the fact that the gluon "decays" to a massive jet may indicate that we should include mass spectrum effects and thresholds in the phase space calculations. Such effects could distort simple QCD predictions; e.g., the $\Upsilon \to \gamma gg/ggg$ ratio will be enhanced. We also note that higher order (in α_s) channels $\Upsilon \to gq\bar{q}$ and $q\bar{q}$ could be relatively more important than indicated by perturbation theory if the gluon jet has an effectively heavier mass spectrum than the quark jet.[61]

To summarize, let us list the discriminants which could distinguish quark and gluon jets:

(a) Multiplicity. As discussed in Section 6, color octet separation leads to multiplicity of soft gluons and sea quarks 9/4 as large as color triplet separation.[3,4] If this translates into higher hadron multiplicity, then $\Upsilon \to 3g$ decay events with low sphericity will have a higher rapidity plateau in the central region with respect to the $g + (gg)$ jet axis.

(b) Leading particles. If we trust lowest order QCD perturbation theory, then the distribution of charged particles as $x \to 1$ falls off faster in gluon jets compared to hadron jets. A simple form which has the predicted $x \to 0$ and $x \to 1$ limiting behavior is[3,62]

$$D_{H^\pm/g}(x) = \frac{9}{8}\left[D_{H/q}(x) + D_{H/\bar{q}}(x)\right](1-x) \tag{7.3}$$

Gluon jets, however, may have enhanced number of $I = 0$ states at $x \to 1$ which have a strong gluon component, e.g., $g \to \eta, \omega, \psi$, etc.[63]

(c) Quantum numbers. The total charge of the jet in its fragmentation region is related to the charge of the parent as discussed in Section 6.

(d) Transverse momentum distribution. Gluon jets should be more diffuse (large $\langle k_T^2 \rangle$) than quark jets because of the increased number of soft gluon interactions (increased "straggling").[43,44] This effect also results if the gluon decays to $q\bar{q}$ before color neutralization occurs.

(e) Gluon jets may be "oblate." It is possible that the (linear) polarization of a gluon is reflected by the distribution of hadrons in the jet. This possibility is discussed in detail in a recent paper by DeGrand and Schwitters and myself.[7]

For example, suppose that hadrons are produced from gluon jets after the decay $g \to q\bar{q}$. Then by convolution,

$$G_{H/g}(z,\phi) \cong \int_z^1 \frac{dx}{x}\, G_{H/q}\left(\frac{z}{x}\right) G_{g/q}(x,\phi) + (q \to \bar{q}) \ . \tag{7.4}$$

In lowest order perturbation theory spin 1/2 quarks from $g \to q\bar{q}$ are aligned with respect to the gluon linear polarization:

$$G_{q/g}(x,\phi) \propto [1 - 4\cos^2\phi \; x(1-x)]$$

$$\cos\phi = \hat{q} \cdot \hat{\varepsilon} \tag{7.5}$$

This then implies a sum rule for the momentum weighted distribution of hadrons:

$$\frac{d\varepsilon}{d\phi} \equiv \sum_H \int_0^1 dz \; z \; D_{H/g}(z,\phi)$$

$$= \frac{1}{4\pi}\,(1 + 2\sin^2\phi) \quad . \tag{7.6}$$

In this model, hadrons are 3 times more likely to be produced orthogonal rather than parallel to $\hat{\varepsilon}$, thus producing a non-cyclindrical "oblate" jet. Oblateness can be determined experimentally by finding the principal axes of $\sum_H p_i^H p_j^H$ as in sphericity analyses.

Equation (7.6) should be regarded as an upper limit to the oblateness effect in QCD, since (1) not all hadrons arise from the q and $\bar{q}$ decay products, and (2) the "straggling" from $g \to g_{soft} + g$ due to soft gluon emission depolarizes the gluon. The latter effect is of order $\alpha_s(s)$ and can probably be diminished by selecting events with fast hadrons. The main problem is that gluons are not produced 100% linearly polarized in a given direction.

For example, in $\eta(Q\bar{Q}) \to g+g \to q\bar{q} + q\bar{q}$ (pseudoscalar decay analogue of π^0 double Dalitz decay), the correlation between gluon polarizations is

$$\frac{dN}{d\psi} = \frac{1}{9\pi}\,(4 + \sin^2\psi) \tag{7.7}$$

and

$$\frac{d\varepsilon}{d\psi} \equiv \sum_{H_a,H_b} \int_0^1 dz_a \int_0^1 dz_b \; \frac{dN}{dz_a\, dz_b\, d\psi}\, z_a\, z_b$$

$$= \frac{15 + 2\sin^2\psi}{32\pi} \tag{7.8}$$

gives the summed correlation between hadrons of the two jets. The maximal effect is only 13%. Similarly in $\underline{\gamma} \to 3q$, the polarization of each gluon is correlated with the normal to the decay plane. Summing over hadrons (from $g \to q\bar{q} \to \text{hadrons} + q + \bar{q}$) gives

$$\frac{d\varepsilon}{d\chi} = (X_1^2 + X_2^2 + X_3^2) + \frac{1}{4}(1 - 2\cos^2\chi)\, X_1 X_2 X_3 \tag{7.9}$$

where $\cos\theta_{23} = 1 - X_1$ is the cosine of the angle between the gluon jets, and $\cos\chi = p_{\hat{H}} \cdot \hat{n}$ is the projection of the hadron direction with the decay plane normal. The maximal effect occurs for $\theta_{ij} = 120^\circ$ ("tripod" configuration), where we predict that a hadron is 9/7 more likely to be aligned in the plane than normal to the plane.

Finally, for $e^+e^- \to q\bar{q}g$ or $eq \to eq'g$ events, the distribution of gluon polarization is given by

$$\begin{aligned} z\frac{dN}{dz\, d\phi\, d^2k_T} &= zG_{g/q}(z, \phi, \vec{k}_T^2) \\ &\sim \frac{4}{3}\frac{\alpha_s}{\pi^2}\left[z^2 + 4(1-z)\cos^2\phi\right]\frac{\vec{k}_T^2}{(\vec{k}_T^2 + z^2 m_q^2)^2} \end{aligned} \tag{7.10}$$

where $\cos\phi = \hat{\varepsilon}\cdot\hat{n}$ and n is in the plane of $q\bar{q}$ or qq'. The average over ϕ gives the standard $1 + (1-z)^2$ distribution.

Although these model calculations give only a first estimate, it seems likely that the spin-1 nature of the gluon in QCD will be reflected in the oblateness of the distribution of its decay products.

8. The Gluon Distribution in Hadrons[8]

Another important question concerning the hadron wavefunction is the nature of its gluon distribution. In QCD, there are three essentially different sources of gluons within a meson or baryon, as discussed in Chapter II.

Often only gluons from quark bremsstrahlung (type (a)) have been taken into account in the standard QCD phenomenological analyses: one assumes that at some Q_0^2 the proton only consists of valence quarks, and that the gluons and sea quarks can be generated by QCD evolution equations for $Q^2 \neq Q_0^2$. In such an approach the probability distribution for quarks is sufficient to determine the probability distribution for gluons. Only "diagonal" terms are computed; off-diagonal diagrams involving two quarks are not considered. This analysis reproduces the q^2-dependent QCD moments for structure functions.[64]

However, for x and $\vec{k}_T \to 0$ (the long wavelength limit) the gluon only "sees" a color singlet source; thus there must be coherent cancellations between the different quark currents. The diagonal approximation can only be accurate for large transverse momentum gluons (see Fig. 14).

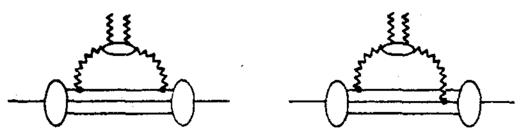

Fig. 14. Contributions to quark sea from (a) diagonal, and (b) off-diagonal gluon contributions. Only (a) is considered in usual analyses.

Gunion and I[7] have recently considered a simple gauge theory model of the meson which preserves gauge invariance and allows a detailed study of the color coherence effects. (The same physics also occurs in QED when one determines the photon distribution in a neutral atom, such as positronium). In the model, the gluon distribution can be computed in lowest order analytically for all x and k_T. For small x, we find

$$G_{g/M}(x,\vec{k}_T^2) = \frac{8}{3}\frac{\alpha_s}{\pi^2}\frac{1}{x}\frac{1}{\vec{k}_T^2}\left[1 - F_M\left(\frac{\vec{k}_T^2}{(1-\bar{x}_q)^2}\right)\right] \tag{8.1}$$

where $F_M(Q^2) \cong 1/(1+Q^2/M_V^2)$ is the meson electromagnetic form factor. The first term in the bracket is the usual (diagonal) contribution obtained from the convolution of $G_{q/M}$ or $G_{\bar{q}/M}$ with $G_{g/q}$. The F_M term from the (off-diagonal) coherence of the q and $\bar{q}$ distributions is only unimportant at large $k_T^2 \gg (1-\bar{x}_q)^2 M_V^2$, where $\bar{x}_q \cong 1/2$ is the average momentum fraction of the quark in the meson, and M_V sets the scale of the electromagnetic form factor and hadron size. The coherence of the color singlet bound state eliminates the usual infrared divergences at $\vec{k}_T^2 \to 0$. In this simple model, the standard denominator for a quark target $(\vec{k}_T^2 + x^2 m_q^2)^{-1}$ is replaced by $(\vec{k}^2 + M_V^2)^{-1}$; i.e., there is no quark mass singularity for $m_q \to 0$.

The most important consequence for phenomenology is the fact that the gluon distribution in a hadron reflects its size and constituency. The gluon momentum and sea quark fractions will be bigger the larger the size (λ_H) of the hadron $xG_{g/H}(x) \sim \log\left[(1 + \lambda_H^2\, k_{T\max}^2)\right]$. In addition, the gluon distribution in a hadron clearly tends to increase with the number of quark constituents. Eventually, at large enough log q^2 the QCD radiative corrections will cause the structure functions to contract to the $x \sim 0$ region, and the gluon and quark momentum fractions will reach an asymptotic equilibrium independent of the nature of the target. However, in the preasymptotic domain, target effects are important for determining the gluon and sea-quark distributions. A number of applications are discussed in Ref. 7 including the prediction that the gluon momentum fraction in mesons at present q^2 is appreciably smaller than in nucleons. This prediction can be tested in reactions such as ψ production or gluon jet production in hadronic collisions, where a gluon-induced subprocess is expected to play a major role.[65]

The models used thus far for the gluon distribution in hadrons are primitive and can only take into account perturbative effects. Non-perturbative claculations which can account for final state interaction effects, and higher Fock state components in the bound state wavefunction will be required before a definitive prediction of the gluon distribution in a hadron can be made.

9. Conclusions

Although there are tantalizing hints of success, there is as yet no convincing quantitative evidence that inclusive hadronic reactions are described by perturbative quantum chromodynamics. A great deal of experimental and theoretical work will be required to provide bona fide tests of the theory at even the 10-20 percent level. Among the outstanding problems:

(1) The production cross section for jets in hadron-hadron collisions is not known to within a factor of 2 or 3, let alone its scaling properties at fixed x_T and θ_{cm}. If the combined QCD plus CIM description given here is correct, the jet/π cross section should increase as $\sim p_T^2$ at fixed x_T and θ_{cm} for $p_T \gtrsim 4$ GeV/c. Scale breaking due to QCD radiative corrections are discussed in Chapter II. The k_T smearing effect for $p_T > 4$ GeV/c changes the predictions by less than a factor of 2 if off-shell kinematics are used.[18]

(2) The existence of charge correlations between the trigger and away side hadrons, as observed by the BFS collaboration[25] evidentally eliminate 2 to 2 QCD Born subprocesses as the dominant hard scattering mechanism for single hadron production in the region up to $p_T > 4$ GeV. The extension of these measurements to higher p_T and x_T is critical. Nuclear targets tend to obscure flavor correlations because of charge averaging and final state interactions.

(3) Cross sections for hadron pairs at large $\mathscr{M}^2$ tend to be insensitive to the controversial k_T smearing effect. It is particularly interesting to compare hadron pairs and muon pairs at the same kinematics. One predicts[66]

$$\frac{\dfrac{d\sigma}{d\mathscr{M}^2 dy}\,(pp \to H^+H^-X)}{\dfrac{d\sigma}{d\mathscr{M}^2}\,(pp \to \mu^+\mu^-X)} = \left(\frac{1}{\mathscr{M}^2}\right)^k f\left(y\,,\, \frac{\mathscr{M}^2}{s}\right) \tag{9.1}$$

where $k = 2$ for meson pairs and $k = 4$ for baryon pairs. If 2 to 2 QCD diagrams are dominant, then $k = 0$, and there are only minor scale violations from the relevant structure functions and an overall factor of $[\alpha_s(\mathscr{M}^2)/\alpha]^2$.

(4) It is very important that QCD predictions for direct high p_T photon reactions be tested, starting with the original Bjorken-Paschos[67] inelastic Compton reaction $\gamma p \to \gamma X$ and inclusive photoproduction $\gamma p \to \pi X$ (reactions without forward hadrons) to direct photon production $pp \to \gamma X$, two photon processes $\gamma\gamma \to X$, $e^+e^- \to \gamma + \pi^\pm + X$ (charge asymmetry), and $e^\pm p \to e^\pm \gamma X$ ($e^\pm$ asymmetry).[1,2] The photon is the only non-colored elementary field that directly participates in QCD dynamics at short distances; unless its pointlike couplings to quarks are confirmed, predictions for perturbative processes involving gluons are probably meaningless. The close relationship between photon production to gluon and quark jet production is discussed in Section 5. We also note the remarkable fact that the asymptotic photon structure function is scale-invariant up to an overall factor of $\alpha_s^{-1}(p_T^2)$, and photon-induced cross sections such as $Ed\sigma/d^3p\,(\gamma\gamma \to \text{Jet} + X)$ are asymptotically scale free and independent of $\alpha_s(p_T^2)$ when perturbative contributions to all orders are included (see Chapter III).

(5) The complete picture of quark and gluon distributions in hadrons will require attention to coherent effects and multiparticle correlations, as discussed in Section 8. Measurements of the final states in deep inelastic processes and massive lepton pair production processes, together with comparisons with low q^2 and low $\mathcal{M}^2$ events, can give detailed information on the evolution of multiquark and gluon jets, including the effect of color separation, "hole" parton production, and the influence of nuclear targets.

(6) Perhaps the most convincing evidence for underlying scale-invariant quark interactions comes from large momentum transfer exclusive measurements such as the form factors at large t and hadron scattering and photoproduction at large t and u.

As we have discussed in Chapter II, this is potentially the most important testing ground of the dynamics and symmetry properties of QCD.

References

1. C. O. Escobar, DAMTP 78/9 (1978); G. R. Farrar and S. C. Frautschi, Phys. Rev. Lett. 36, 1017 (1976); and J. D. Bjorken et al., Phys. Rev. D4, 3388 (1971). An indication that the interactions of large transverse moment real photon have point-like interactions is given by the measurements of the $e^+ - e^-$ asymmetry is deep inelastic bremsstrahlung by D. L. Fancher et al., Phys. Rev. Lett. 38, 800 (1977). See also S. J. Brodsky, J. F. Gunion and R. L. Jaffe, Phys. Rev. D6, 2487 (1972).

2. R. Rückl, S. J. Brodsky and J. Gunion, SLAC-PUB-2115 (to be published in Phys. Rev.); F. Halzen and D. Scott, Phys. Rev. Lett. 40, 1117 (1978); and H. Fritzsch and P. Minkowski, Phys. Lett. 63B, 99 (1976).

3. S. J. Brodsky and J. F. Gunion, Proceedings of the 7th International Collisions on Multiparticle Practions, Munich (1976); and Phys. Rev. Lett. 37, 402 (1976).

4. K. Konishi, A. Ukawa and G. Veneziano, CERN-TH-2509 (1978).

5. T. DeGrand, Y. J. Ng and S. H. H. Tye, Phys. Rev. D16, 3251 (1977); K. Koller, H. Krasemann and T. F. Walsh, DESY 78137 (1978); K. Koller and T. Walsh, 781/6 (1978); and A. DeRujula, J. Ellis, E. G. Floratas and M. K. Gaillard, CERN preprint TH-2455 (1978).

6. S. J. Brodsky, D. G. Coyne, T. A. DeGrand and R. R. Horgan, Phys. Lett. 73B, 203 (1978).

7. S. J. Brodsky, T. A. DeGrand and R. F. Schwitters, SLAC-PUB-2160 (1978) (to be published in Phys. Lett.).

8. S. J. Brodsky and J. F. Gunion, SLAC-PUB-2163 (1978).

9. D. Sivers, R. Blankenbecler and S. J. Brodsky, Phys. Reports 23C:1 (1976); and M. Jacob and P. V. Landshoff (to be published in Phys. Reports).

10. R. D. Field, CALT-68-683 (presented at the XIX International Conference on High Energy Physics, Tokyo, 1978, and references therein).

11. R. Cutler and D. Sivers, Phys. Rev. D16, 679 (1977) and Phys. Rev. D17, 196 (1978); and B. L. Combridge, J. Kripfganz and J. Ranft, Phys. Lett. 234 (1977).

12. R. Blankenbecler, S. J. Brodsky and J. F. Gunion, Phys. Rev. D18, 900 (1978); and P. V. Landshoff and J. C. Polkinghorne, Phys. Rev. D8, 927 (1973), and Phys. Rev. D10, 891 (1974).

13. We cavalierly refer to subprocesses which involve more than the minimum number of external fields as "high twist".

14. S. J. Brodsky and G. Farrar, Phys. Rev. D11, 1309 (1975).

15. Note, however that the standard QCD corrections to the structure functions $G_{a/A}(x,Q^2)$ depend on the color Casmir operators of a and thus vanish if the constituent is a color singlet (see Chapter II).

16. S. D. Ellis, M. Jacob and P. V. Landshoff, Nucl. Phys. B108, 93 (1976). See also J. D. Bjorken and G. R. Farrar, Phys. Rev. D9, 1449 (1974).

17. P. V. Landshoff, J. C. Polkinghorne and R. D. Short, Nucl. Phys. B28, 222 (1971); and S. J. Brodsky, F. E. Close and J. F. Gunion, Phys. Rev. D8, 3678 (1973).

18. For an extensive discussion see W. E. Caswell, R. R. Horgan and S. J. Brodsky, SLAC-PUB-2106 (to be published in Phys. Rev.). Detailed calculations for QCD subprocesses are given by R. R. Horgan and P. Scharbach, SLAC-PUB-2188 (1978). The importance of off-shell kinematics in calculating k_T fluctuations has also been discussed by K. Kinoshita and Y. Kinoshita, KYUSHU-78-HE-6 (1978); M. Chase, DAMTP 77/29 (1977); and R. Raitio and R. Sosnowski, HU-TFT-77-22 (1977).

19. R. Blankenbecler, S. J. Brodsky and J. F. Gunion, Ref. 12, and Phys. Rev. D6, 2652 (1972).

20. S. J. Brodsky and G. Farrar, Phys. Rev. Lett. 31, 1/53 (1973); and V. A. Matveev, R. M. Muradyan and A. N. Tavkheldize, Lett. Nuovo Cimento 7, 719 (1973).

21. D. Antreasyan et al., preprint EFI 78-29 (1979), and Phys. Lett. 38, 112 (1977); and J. W. Cronin et al., Phys. Rev. D11, 3105 (1975). See also M. Shochet, Proceedings of the XVIII International Conference on High Energy Physics, Tblisi (1976).

22. A. G. Clark et al., Phys. Lett. 74B, 267 (1978). CERN-Columbus-Oxford-Rockefeller Expt., reported by L. Di Lella in Workshop on Future ISR Physics, September (1977), edited by M. Jacob.

23. D. Jones and J. F. Gunion, SLAC-PUB-2157 (1978).

24. R. P. Feynman, R. D. Field and G. C. Fox, Nucl. Phys. B128, 1 (1977); R. D. Field and R. P. Feynman, Phys. Rev. D15, 2590 (1977); R. Baier, J. Cleymans, K. Kinoshita and B. Peterson, Nucl. Phys. B118, 139 (1977); and J. Kripfganz and J. Ranft, Nucl. Phys. B124, 353 (1977).

25. M. G. Albrow et al., NBI preprints (1978); R. Moller, Symposium on Jets in High Energy Collisions (1978); and K. H. Hansen, presented to the XIX International Conference on High Energy Physics, Tokyo (1978), and Nucl. Phys. B135, 461 (1978).

26. R. P. Feynman, R. D. Field and G. C. Fox, CALT-68-651 (1978). See also A. P. Contogouris, R. Gaskell and S. Papadopoulos, Phys. Rev. D17, 2314 (1978); A. P. Contogouris, McGill preprint (1978); J. F. Owens and J. D. Kimel, FSU-HEP-780330 (1978); J. F. Owens, FSU-HEP-780609 (1978), and Phys. Lett. 76B, 85 (1978); J. Ranft and G. Ranft, preprints KMU-HEP-7806 and 7805 (1978), and Lett. Nuovo Cimento 20, 669 (1979); and M. Fontannaz, Nucl. Phys. B132, 452 (1978).

27. A simplified analysis of charge correlations is given in S. J. Brodsky, Proceedings of the VII International Symposium on Multiparticle Dynamics, Kaysersberg, France, June (1977). An analysis of the QCD Born subprocesses is given by R. P. Feynman et al., Ref. 26.

28. R. J. Fisk et al., Phys. Rev. Lett. 40, 984 (1978).

29. J. D. Bjorken and J. B. Kogut, Phys. Rev. D8, 1341 (1973).

30. Y. L. Dokshitser, D. I. Dyakanov and S. I. Troyan, SLAC-TRANS-0183, Trans. from Proceedings of the 13th Leningrad Winter School on Elementary Particle Physics (1978); Leningrad preprint (1978).

31. J. C. Vander Velde, presented at the Symposium on High Energy Collisions, Niels Bohr Institute and Nordita, July (1978) (to be published in Physica Scripta); and J. S. Bell et al., UMBC-9 (1978).

32. This point has been emphasized by W. Ochs and L. Stodolsky (unpublished).

33. F. Witten, Nucl. Phys. B120, 189 (1977); and W. Frazer and J. F. Gunion, UCSD preprint 10P10-194 (1978).

34. M. Fontannaz, Phys. Rev. D14, 3127 (1976).

35. M. Duong-van, K. V. Vasavada and R. Blankenbecler, Phys. Rev. D16, 1389 (1977).

36. C. M. Debeau and D. Silverman (to be published) have given a combined QCD + CIM calculation of the massive lepton pair transverse momentum distribution.

37. C. Bromberg et al, Phys. Rev. Lett. 38, 1447 (1977), and Nucl. Phys. B134, 189 (1978); and M. D. Corcoran et al., presented at the XIX International Conference on High Energy Physics, Tokyo (1978).

38. J. K. Cobb *et al.*, CERN preprint 78-0925 (1978).

39. A. Casher, J. Kogut and L. Susskind, Phys. Rev. Lett. 31, 792 (1973).

40. J. Bjorken, SLAC-PUB-1756, Lectures given at the International Summer School in Theoretical Physics, DESY (1975).

41. S. J. Brodsky and N. Weiss, Phys. Rev. D16, 2325 (1977).

42. G. R. Farrar and J. Rosner, Phys. Rev. D7, 2747 (1973); J. L. Newmeyer and D. Sivers, Phys. Rev. D9, 2592 (1974); and R. Cahn and E. Colglazier, Phys. Rev. D9, 2592 (1974).

43. K. Shizuya and S. H. H. Tye, Fermilab-PUB-78/54 (1978).

44. M. Einhorn and B. Weeks, SLAC-PUB-2164 (1978).

45. A. Casher, H. Neuberger and S. Nussinov, Tel Aviv preprint TAUP-694-78 (1978).

46. J. Bjorken, Phys. Rev. D7, 282 (1973).

47. See Refs. 3, 19, and 41.

48. S. J. Brodsky, J. F. Gunion and J. Kühn, Phys. Rev. Lett. 39, 1120 (1977).

49. S. J. Brodsky and R. Blankenbecler, Phys. Rev. D10, 2973 (1974).

50. W. Ochs, MPI-PAE/PTH 33/77 (1977), Proceedings of the 12th Rencontre de Moriond, Flaine (1977), and Nucl. Phys. B118, 397 (1977).

51. H. Goldberg, Nucl. Phys. B44, 149 (1972).

52. J. C. Sens *et al.*, CHLM Colloboration (unpublished).

53. S. J. Brodsky and J. F. Gunion, Phys. Rev. D17, 848 (1978).

54. If the spin of the leading particle does not match that of the projectile, we expect an additional suppression factor $(1-x)^{2|S_z^a - S_z^A|}$. S. J. Brodsky, J. Gunion, N. Fuchs and M. Scadron (to be published).

55. E. E. Kluge *et al.* (CCHK Collaboration), presented at the Symposium on Jets in High Energy Collisions, Niels Bohr Institute and Nordita, July (1978) (to be published in Physica Scripta); and D. Drijard *et al.*, CERN/EP/Phys. 78-14 (1978).

56. K. P. Das and R. C. Hwa, Phys. Lett. 68B, 459 (1977), and 73B, 504 (1978).

57. T. A. DeGrand and H. I. Miettinen, Phys. Rev. Lett. 40, 612 (1978); and T. A. DeGrand, SLAC-PUB-2182 (1978).

58. S. J. Brodsky, W. Caswell and R. Horgan (unpublished). See S. J. Brodsky, SLAC-PUB-1937, Proceeding of the 12th Recontre de Moriond, Flaire (1977).

59. M. Chanowitz, Phys. Rev. D12, 918 (1975); and L. Okun and M. Voloshin, ITEP-95 (1976).

60. V. A. Novikov et al., Phys. Report 41C, 1 (1978).

61. S. J. Brodsky, M. Dine and E. Fahri (in progress).

62. S. J. Brodsky, Ref. 58.

63. H. Fritzsch and K. H. Streng, CERN-TH-2520 (1978).

64. See, e.g., A. Buras and K. Gaemer, Nucl. Phys. B132, 249 (1978). For a detached discussion of the diagonal approach see F. Martin, SLAC-PUB-2192 (1978).

65. S. Ellis and M. Einhorn, Phys. Rev. D12, 2007 (1975), and Phys. Rev. Lett. 36, 1263 (1976); and C. Carlson and R. Suaya, Phys. Rev. D14, 3115 (1976), and Phys. Rev. D18, 760 (1978).

66. R. Blankenbecler and S. J. Brodsky (unpublished).

67. J. D. Bjorken and E. Paschos, Phys. Rev. 185, 1975 (1969).

Acknowledgements

Parts of these lectures overlap with material presented at the Symposium on Jets in High Energy Collisions (Copenhagen, July 1978; SLAC-PUB-2217), the Joseph M. Weis Memorial Symposium on Strong Interactions, University of Washington, November 1978; SLAC-PUB-2240), and the Workshops on High Energy Physics (Cal Tech, February 1979; SLAC-PUB-2294).

Chapter II was written in collaboration with G. Peter Lepage. The new applications of QCD to exclusive processes are based on work done with Lepage and also with Y. Frishman and C. Sachrajda, and I am grateful to them for many helpful conversations.

A large part of these lectures are based on collaborations with many other colleagues, including E. Berger, R. Blankenbecler, C. Carlson, W. Caswell, G. Farrar, T. DeGrand, J. Gunion, R. Horgan, H. Lipkin, R. Rückl, R. Schwitters, and N. Weiss. I wish to thank them and the participants at the La Jolla Workshops for many helpful discussions.

I am also grateful to William Frazer, the organizer of these workshops, for his assistance and hospitality.